

**Effects of the Matrix Metalloproteinase Inhibitor  
Batimastat on Individual Stages of Metastasis**

by

**J. Stewart M. Wylie  
Department of Medical Biophysics**

**Submitted in partial fulfillment  
of the requirements for the degree of  
Master of Science**

**Faculty of Graduate Studies  
The University of Western Ontario  
London, Ontario  
April 23, 1997**

**© Copyright Stewart Wylie, 1997**



National Library  
of Canada

Acquisitions and  
Bibliographic Services

395 Wellington Street  
Ottawa ON K1A 0N4  
Canada

Bibliothèque nationale  
du Canada

Acquisitions et  
services bibliographiques

395, rue Wellington  
Ottawa ON K1A 0N4  
Canada

*Your file* *Votre référence*

*Our file* *Notre référence*

**The author has granted a non-exclusive licence allowing the National Library of Canada to reproduce, loan, distribute or sell copies of his/her thesis by any means and in any form or format, making this thesis available to interested persons.**

**The author retains ownership of the copyright in his/her thesis. Neither the thesis nor substantial extracts from it may be printed or otherwise reproduced with the author's permission.**

**L'auteur a accordé une licence non exclusive permettant à la Bibliothèque nationale du Canada de reproduire, prêter, distribuer ou vendre des copies de sa thèse de quelque manière et sous quelque forme que ce soit pour mettre des exemplaires de cette thèse à la disposition des personnes intéressées.**

**L'auteur conserve la propriété du droit d'auteur qui protège sa thèse. Ni la thèse ni des extraits substantiels de celle-ci ne doivent être imprimés ou autrement reproduits sans son autorisation.**

0-612-21116-9

## **Abstract**

**Matrix metalloproteinases have been implicated in facilitating metastasis. The synthetic matrix metalloproteinase inhibitor batimastat has been shown to inhibit metastasis to mouse lung, but it is not known which stages of the metastatic process are affected. I have shown, for the first time, that batimastat can also reduce metastasis to the mouse liver: daily administration of batimastat during an experimental hematogenous metastasis assay caused a 23.1% decrease in liver tumor size ( $P < 0.05$ ). I then studied the effects of batimastat on three stages of metastasis: extravasation, initial tumor growth, and angiogenesis. Intravital videomicroscopy showed that batimastat did not inhibit extravasation. Examination of liver sections at four days post-injection demonstrated that batimastat did not inhibit initial growth. However, stereological examination of blood vessels in stained sections of 19-day tumors revealed that batimastat significantly reduced vascular density ( $P < 0.05$ ). I conclude that batimastat reduces metastasis to the liver by inhibition of angiogenesis.**

**Keywords:** cancer, metastasis, matrix metalloproteinase inhibitor, batimastat, extravasation, angiogenesis, intravital videomicroscopy.

## **Acknowledgements**

I would like to express my sincere thanks to my supervisor, Dr. Ann Chambers, and my co-supervisor, Dr. Alan Groom, for their support and encouragement through the many trying times that drug testing brings. I would also like to thank the members of my advisory committee, Dr. Ian MacDonald and Dr. Vince Morris, with special thanks to Dr. MacDonald for teaching me everything I know about mouse surgery and how to always see the good side of results, whatever they may be.

I would like to acknowledge the invaluable assistance of Eric Schmidt, who showed me the ropes of intravital videomicroscopy and always had a knack for seeing things that I had missed. I thank Sylvia Hill and Marsha Grattan for teaching and assisting me with tissue culture, and Nancy Kerkvliet for her technical support with my angiogenesis studies. I also thank the members of my research group for their support and humour throughout my graduate work.

I would like to thank British Biotech Pharmaceuticals for their very kind donation of two shipments of batimastat, and the National Cancer Institute of Canada for funding my research.

# TABLE OF CONTENTS

CERTIFICATE OF EXAMINATION .....	ii
ABSTRACT.....	iii
ACKNOWLEDGEMENTS .....	iv
TABLE OF CONTENTS .....	v
LIST OF TABLES .....	vii
LIST OF FIGURES.....	viii
1. INTRODUCTION.....	1
1.1 Cancer .....	1
1.2 The Metastatic Process .....	2
1.3 Matrix Metalloproteinases.....	4
1.4 Batimastat.....	6
1.5 Research Objectives .....	8
1.5.1 Does batimastat inhibit metastasis to the mouse liver?.....	8
1.5.2 What stages of the metastatic process does batimastat inhibit? .....	9
2. MATERIALS AND METHODS .....	11
2.1 Experimental Metastasis Assays .....	11
2.1.1 Cell Culture.....	11
2.1.2 Batimastat .....	11
2.1.3 Metastasis Assays.....	12
2.1.4 Data Analysis .....	13
2.2 Extravasation Assays.....	14
2.2.1 Cell Culture and Fluorescent Labelling.....	14
2.2.2 Extravasation Assay Preparation.....	14
2.2.3 Intravital Videomicroscopy.....	15
2.2.4 Data Analysis .....	18
2.3 Initial Growth Assay .....	18

2.3.1 Cell Culture and Microsphere Addition.....	18
2.3.2 Surgery and Batimastat Administration.....	19
2.3.3 Liver Sectioning.....	19
2.3.4 Growth Assay.....	19
2.3.5 Data Analysis.....	20
2.4 Tumor Angiogenesis Assay.....	20
2.4.1 Tissue Fixation and Embedding.....	20
2.4.2 Tissue Staining.....	21
2.4.3 Angiogenesis Assay.....	21
2.4.4 Data Analysis.....	23
3. RESULTS.....	24
3.1 Experimental Metastasis Assays.....	24
3.2 Extravasation Assays.....	26
3.3 Initial Growth Assay.....	31
3.4 Angiogenesis Assay.....	35
4. DISCUSSION AND CONCLUSIONS.....	40
4.1 Metastasis to the Mouse Liver.....	40
4.2 Extravasation from Liver Sinusoids.....	43
4.3 Initial Growth of Micrometastases.....	45
4.4 Angiogenesis.....	48
4.5 Concluding Remarks.....	51
4.6 Future Considerations.....	52
APPENDIX: ETHICS APPROVAL LETTERS, 1994-1997.....	54
REFERENCES.....	58
VITA.....	63

## **List of Tables**

<b>Table 3.1</b>	<b>19-day experimental metastasis assay, regimen 1</b> .....	<b>25</b>
<b>Table 3.2</b>	<b>19-day experimental metastasis assay, regimen 2</b> .....	<b>25</b>
<b>Table 3.3</b>	<b>Initial growth assay</b> .....	<b>32</b>

## List of Figures

Figure 1.1 The process of hematogenous metastasis.....	3
Figure 2.1 Schematic of intravital videomicroscopy.....	17
Figure 3.1(a) 8 hour IVVM extravasation assay.....	27
(b) 24 hour IVVM extravasation assay.....	27
(c) 48 hour IVVM extravasation assay.....	28
Figure 3.2 IVVM images of cells in the liver microcirculation	
(a) An intravascular B16F1 cell.....	29
(b) A B16F1 cell in the process of extravasation.....	29
(c) Two extravasated B16F1 cells.....	30
Figure 3.3 A B16F1 cell and a 10.2 $\mu\text{m}$ microsphere in a 30 $\mu\text{m}$ section of mouse liver tissue at 4 days p.i.	
(a) View of the cell and microsphere using fibre optic transillumination and fluorescence illumination.....	33
(b) View of the cell and microsphere using fluorescence illumination only .	33
Figure 3.4 A micrometastasis in a 30 $\mu\text{m}$ section of mouse liver tissue at 4 days p.i. .	34
Figure 3.5 Vascular density in liver tumors of varying diameter.....	37
Figure 3.6 A composite image of a one millimetre tumor from the control group at 19 days p.i.....	38
Figure 3.7 Interior of two 1-millimetre tumors at 19 days p.i.	
(a) Interior of a 1-millimetre control tumor.....	39
(b) Interior of a 1-millimetre batimastat-treated tumor.....	39

## **Chapter 1: Introduction**

### **1.1 Cancer**

Cancer is one of the most feared diseases, due to its high rates of occurrence and mortality. In 1996, an estimated 129 200 Canadians developed cancer, and 61 800 Canadians died of the disease. A Canadian male has a 1 in 2.4 chance of developing cancer in his lifetime, and a 1 in 4 chance of dying of cancer. A Canadian female is slightly less at risk, with odds of 1 in 2.7 and 1 in 5, respectively. Although older people are at greater risk of developing the disease, cancer occurs frequently in males and females of all ages. With 55% of new cases of cancer and 44% of cancer deaths occurring in people under the age of 70, cancer is the leading cause of premature mortality in Canada (1).

Tumors occur with great frequency, especially in older animals and humans. A tumor arises when growth regulation is lost in a cell, which then begins to divide uncontrollably. Most tumors are benign and pose little risk to their hosts, as they are localised, composed of well differentiated cells, and are often separated from surrounding normal tissue by a fibrous capsule. Warts are a common example of benign tumors. Tumors are life-threatening if their cells have the ability to invade the surrounding tissue to expand the tumor mass or to form new tumors; such a tumor is malignant and is termed a cancer. Many types of malignant tumors contain cells capable of invading lymphatic vessels or the blood circulation, travelling to distant sites in the body, and growing into new tumors at these sites. This process of invasion, spread, and growth is termed metastasis.

## 1.2 The Metastatic Process

Cancer metastasis is the major cause of treatment failure in cancer patients, as the primary tumor can normally be removed to cure patients in whom metastasis has not yet occurred. Metastases are also often very difficult to detect, and it is likely that many undetectable metastases may in fact be present at the time of primary tumor treatment. Small metastases or even single cancer cells may lay dormant throughout the body for many years, until they are stimulated to grow and kill their hosts. It is clear, then, that great strides would be made in cancer treatment if the progression of metastasis could be suppressed.

Metastasis is a process consisting of several discrete stages (2-4, and Figure 1.1). To begin, a metastatic cell from the primary tumor must invade host tissue barriers adjacent to the tumor, and subsequently invade the vascular wall of lymphatic channels or blood vessels in order to disseminate. Once in the circulation, the cell is swept along by the blood flow until it becomes arrested by size restriction in the capillary bed of the target organ. The cell must then exit the circulation, or *extravasate*, by again invading through the vascular wall. The extravascular cell then migrates a short distance through the connective tissue of the extracellular matrix, until it finds a suitable location to begin growth into a secondary metastatic tumor. The tumor continues to grow until the oxygen demand by the cells in its interior is more than can be supplied by diffusion from the tumor exterior; normally this occurs when the tumor is about one or two millimetres in diameter (5). In order to continue growing, the tumor must recruit host endothelial cells in order to construct new blood vessels within itself, a process called angiogenesis. With oxygen supplied to its interior cells, the tumor may grow until the host is dead.

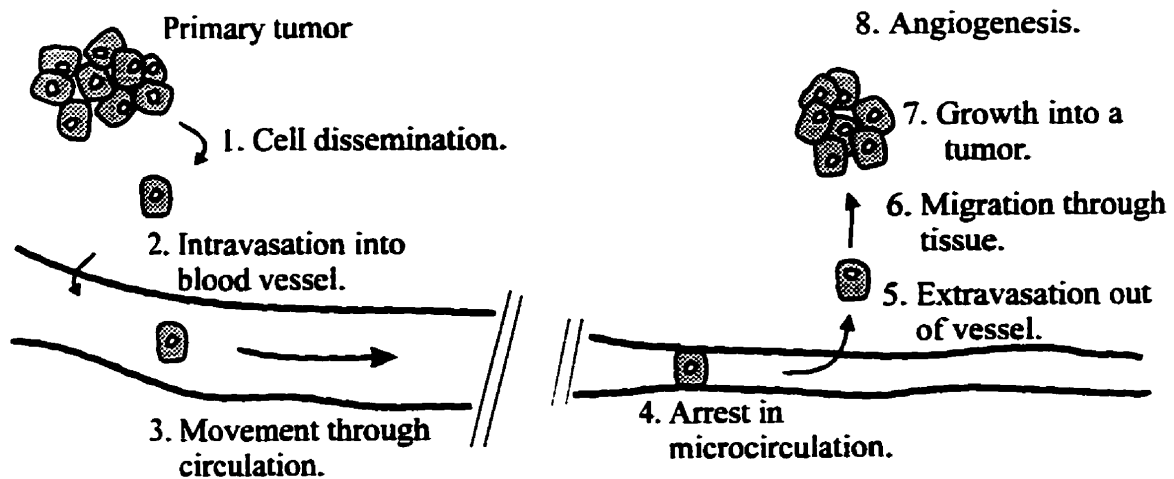


**Figure 1.1** The process of hematogenous metastasis depicted in eight stages. In some cases, the blood vessel into which the tumor cell intravasates may be within the primary tumor, as a result of angiogenesis to facilitate tumor growth. Secondary angiogenesis (stage 8) is not illustrated, but occurs by endothelial cell migration and vessel formation within the tumor when the tumor is 0.2-2 mm in diameter.

Metastasis is a very inefficient process, as only a small fraction of the cells shed from a primary tumor succeed in forming secondary metastatic lesions (6, 7). This is so because the cells face considerable challenges along the way, the greatest of which are thought to be the numerous tissue barriers which the cells must penetrate. The two most common tissue barriers are the basement membrane of circulatory vessels, and the extracellular matrix which gives rigid structure to tissues. Both of these structures are composed mainly of collagen, laminin, gelatin, and fibronectin. It is logical, therefore, that members of the four families of protein-degrading enzymes, or proteinases, have been shown to facilitate metastasis for cancer cells. These four families include cysteine proteinases, serine proteinases, aspartyl proteinases, and matrix metalloproteinases.

### 1.3 Matrix Metalloproteinases

Matrix metalloproteinases (MMPs) comprise a family of degradative enzymes with at least fifteen members (8-10) traditionally divided into three general subclasses: (a) interstitial collagenase; (b) stromelysins; and (c) gelatinases (type IV collagenases) (11-15). Interstitial collagenase degrades type I collagen and fibrillar collagens II, III, and X. The stromelysins degrade proteoglycan core protein, laminin, fibronectin, gelatin, and the nonhelical portions of basement membrane collagens. Gelatinases degrade type IV collagen, which is the main structural protein of basement membrane, as well as collagen types V, VII, IX, and X, fibronectin, and elastin (12, 13). All MMPs have the following features in common: (a) they are produced and secreted in an inactive, proenzyme form; (b) they have two  $Zn^{++}$  atoms, including one at the active site; and (c) they have two  $Ca^{++}$  ions essential for the stability of the enzyme (11, 13). MMPs are normal cell components that play a key role in tissue remodelling during wound healing (16), embryo implantation (17), and angiogenesis (11, 15, 18).

Significant evidence exists implicating matrix metalloproteinases in tumor invasion and metastasis formation (19). Correlative studies of MMP expression in human tumors indicate MMPs as important components of the invasive phenotype of breast (20, 21), prostate (22, 23), colon (24), lung (25, 26), ovarian (27), and thyroid (28) cancers. In particular, the MMP gelatinase A is associated with invasiveness: most invasive colonic, gastric, ovarian, and thyroid adenocarcinomas or the desmoplastic stroma of breast lesions have been shown to be immunoreactive for gelatinase A, whereas benign proliferative disorders of the breast and colon, normal colorectal and gastric mucosa, and benign ovarian cysts show decreased or negative staining for this enzyme (12, 29-31). MMPs are

normal components of many tissues; it is their uncontrolled overexpression that contributes to the metastatic phenotype. With such convincing evidence mounting, it is clear that MMPs represent a key target in the development of antimetastatic therapies.

Matrix metalloproteinases may be equally important at more than one stage of the metastatic process. Early studies suggested that extracellular proteases are necessary for tumor cells to penetrate the vascular basement membrane; this ability typically distinguishes an invasive carcinoma from a carcinoma *in situ* (11, 32). More recently, it has become clear that degradation of the extracellular matrix as well as basement membrane is required when invasive tumor cells penetrate tissues, enter the circulation (intravasate), and exit the circulation (extravasate) (11). Proteolysis of the surrounding tumor stroma, composed chiefly of extracellular matrix proteins, may be necessary to give the expanding secondary metastatic tumor room to grow. MMPs contributing to this process may originate from the tumor or the stroma (33). Finally, MMPs may aid angiogenesis (13, 14, 34, 35), which is necessary for tumors to grow to more than 1-2 millimetres in diameter. Angiogenesis involves active proteolytic degradation of the extracellular matrix by host endothelial cells as they migrate towards the growing tumor; MMPs may contribute to this proteolysis. MMPs may also be involved in angiogenesis in a more indirect fashion: recent evidence suggests that MMPs can activate latent transforming growth factor- $\beta$ 1 and mobilize basic fibroblast growth factor; these two growth factors, found in the extracellular matrix, stimulate angiogenesis by inducing the migration of endothelial cells (13). Thus, matrix metalloproteinases may contribute to metastasis at virtually every step in the metastatic process.

## **1.4 Batimastat**

Batimastat (BB-94) is a synthetic matrix metalloproteinase inhibitor manufactured by British Biotech Pharmaceuticals. It is a collagen peptide-based hydroxamic acid which inhibits MMPs by binding to the  $Zn^{++}$  atom at the active site of the enzyme (36, 37). Batimastat is classified as a broad spectrum matrix metalloproteinase inhibitor, with the following  $IC_{50}$ s (the drug concentration which inhibits enzyme activity by 50%) against various MMPs: interstitial collagenase, 3 nM; stromelysin, 20 nM; 72kDa type IV collagenase, 4 nM; 92kDa type IV collagenase, 4 nM; and matrilysin, 6 nM (38).

Batimastat has been shown to inhibit the growth of ovarian carcinoma xenografts in nude mice (33). Seven days after introduction of the xenografts into the peritoneal cavity, the mean mass of the batimastat-treated tumors was only 29.7% of the mean mass of the control tumors. Mean survival of the mice was also greatly prolonged, from 19 days in the control group to 129 days in the treated group. The batimastat-treated tumors had a much thicker encapsulating stroma than control tumors; this may have been due to decreased lysis of the stroma by MMPs. Also, the batimastat-treated tumors, unlike the controls, were completely avascular; possibly due to inhibition of MMP-facilitated angiogenesis.

Batimastat has also inhibited human colon tumor growth in nude mice (39). The effects of the inhibitor were very similar to those observed with ovarian carcinoma: the mass of the primary tumor was greatly reduced, and survival of the mice was prolonged. In addition, batimastat reduced spontaneous metastasis from the tumor; only 2 of 20 treated mice displayed distant metastases, compared to 6 of 18 for control mice.

The studies mentioned above deal particularly with the effects of batimastat on existing primary tumors. In order to determine whether batimastat is able to inhibit metastasis, it must be tested in experimental metastasis assays. An experimental metastasis assay involves injecting a suspension of cancer cells into a specified location or circulation of an animal, and observing the metastatic tumors that result. Experimental hematogenous metastasis involves injecting the cells directly into the *blood* circulation. Batimastat has been shown to reduce experimental hematogenous metastasis to the lung following tail vein injection of cancer cells. Chirivi *et al.* (40) demonstrated that batimastat, when administered at 30 mg/kg i.p. four hours before and one, 24, 48, and 72 hours following the tail vein (i.v.) injection of B16-BL6 murine melanoma cells, reduced the number of lung metastases at 21 days post-injection (p.i.) by 70% compared to controls. Watson *et al.* (41) found that batimastat, when administered at 40 mg/kg i.p. four hours before and one, 24, 48, and 72 hours following the i.v. injection of AP5LV human colorectal tumor cells, did not reduce the number or size of lung tumors at 28 days post-injection; however, when batimastat was given once daily at 40 mg/kg i.p. until day 28, the mean tumor mass in the lung was reduced by 28%, with no effect on tumor number. Finally, Eccles *et al.* (42) recently found that batimastat, when given at 30 mg/kg i.p. four hours before and one, six, 24, 48, and 72 hours following the i.v. injection of HOSP.1P rat mammary carcinoma cells, reduced the number of lung colonies by 80.4% and reduced the total lung tumor mass by 93.5% at 35 days post-injection. In general, batimastat appears to be effective in reducing metastasis to the lung, although the type of inhibition (tumor number or tumor size) seems to vary depending on the cell type.

Batimastat has thus shown promise in inhibiting the metastatic process. Since metastasis is responsible for most cancer treatment failures, this compound could be a valuable addition to current therapies. It is speculated that batimastat could serve as an adjuvant to cytotoxic therapy, reducing metastasis in the intervals between chemotherapy or radiation therapy regimens (36, 39). Batimastat is currently in Phase II clinical trials in the United Kingdom (36); however, no results are available yet. A derivative of batimastat, marimastat (BB-2516), is also in clinical trials, and has shown promise against various cancer types (43-46). Much still needs to be investigated, though, especially concerning the antimetastatic mechanism of action of batimastat. My goal was to determine the stages of the metastatic process that batimastat inhibits.

## **1.5 Research Objectives**

### **1.5.1 Does batimastat inhibit metastasis to the mouse liver?**

Prior to this work, no experimental *hematogenous* metastasis assay had been reported that tested the effectiveness of batimastat in reducing metastasis to the mouse liver. Watson *et al.* (41) had tested the ability of batimastat to inhibit metastasis to the liver when C170HM<sub>2</sub> human colorectal cancer cells were injected into the peritoneal cavity of a mouse (thus not a hematogenous assay). This study showed that batimastat could reduce the number of liver tumors by 65% and the size of liver tumors by 57% compared to controls. The liver was of particular interest because it is one of the most common organs in which clinical metastases (i.e. metastases in cancer patients) appear, and because it is an organ which, in mouse, can be observed in detail using intravital videomicroscopy (IVVM), a technique which allows one to view cancer cells in the microcirculation of a

living animal; this will be elaborated on in the next section. Based on the liver study by Watson *et al.*, and the studies that demonstrated that batimastat could reduce metastasis to the mouse lung, we hypothesized that batimastat would inhibit hematogenous metastasis to the mouse liver. This was investigated by performing experimental metastasis assays in which B16F1 murine melanoma cells were targeted to the liver by injection into a mesenteric vein and batimastat was administered in two different treatment regimens.

#### **1.5.2 What stages of the metastatic process does batimastat inhibit?**

Since the experimental hematogenous metastasis assays (section 1.5.1) demonstrated that batimastat could indeed inhibit metastasis to the mouse liver, it became important to determine the stage of metastasis at which batimastat acts. Knowledge of this could lead to improved therapeutic strategies regarding the dosage and timing of administration of this compound, as the therapeutic target would be more precisely defined.

Batimastat, as a general MMP inhibitor, likely inhibits one or more steps in metastasis that require proteolytic degradation. However, this applies to *most* steps in the process: intravasation and extravasation require invasion through the basement membrane of blood vessels; secondary metastatic growth may require proteolysis of the extracellular matrix to give the tumor room to grow and degradation of the tumor stroma as part of normal stroma turnover; and continued secondary growth requires proteolytic degradation of the basement membrane and extracellular matrix by host endothelial cells to enable angiogenesis to proceed. This list can be reduced slightly, however, with the knowledge

that batimastat also reduces *experimental* metastasis, in which the cancer cells start in the circulation and not within a primary tumor. Therefore, batimastat likely inhibits one or more of the following steps: extravasation, initial or early metastatic growth, and angiogenesis.

We initially hypothesized that batimastat inhibited extravasation. Degradation of the basement membrane has long been thought to be the rate-limiting step in metastasis (47, 48). Eccles *et al.* (42) have proposed that batimastat limits extravasation, based on their findings that batimastat reduced lung tumor colonization in rats by up to 80.4% following a 35-day experimental metastasis assay in which the drug was administered only during the first 72 hours, the period during which extravasation takes place. The effects of batimastat on cancer cell extravasation in mouse liver were therefore studied in our laboratory using intravital videomicroscopy (IVVM). IVVM is a technique recently developed to study the metastatic process in mouse and chick embryo models (49-51). It allows observation of individual cancer cells within intact organs of living animals as the cells progress through the various stages of metastasis. By observing the positions of cancer cells relative to mouse liver sinusoids as a function of time following cell injection and subsequent to batimastat treatment, we set out to determine whether batimastat inhibited extravasation. These studies were continued by examining the effects of batimastat on two major post-extravasation metastatic steps: initial growth (the initial formation of micrometastases) and angiogenesis.

## **Chapter 2: Materials and Methods**

**This study was divided into four sections:**

- (a) Experimental Metastasis Assays
- (b) Extravasation Assays
- (c) Initial Growth Assay
- (d) Angiogenesis Assay

### **2.1 Experimental Metastasis Assays**

#### **2.1.1 Cell Culture**

B16F1 murine melanoma cells were used for all experiments. Cells were maintained at 37°C and 5% CO<sub>2</sub> in  $\alpha$ -Plus Minimal Essential Medium (GIBCO/BRL, Burlington, ON) supplemented with 10% fetal calf serum (Hyclone, Logan, UT). The cells were subcultured every three days with 1% trypsin (GIBCO/BRL) in citrate saline solution (0.015 M trisodium citrate-0.13 M potassium chloride, pH 7.4). Before injection into mice, the cells were tested for membrane integrity by determining the proportion of cells that exclude ethidium bromide (EtBr)(52). Under fluorescence microscopy, any cells that take in EtBr appeared red; if fewer than 90% of cells excluded EtBr, the batch was not used. For these assays, 94.9% of cells excluded EtBr.

#### **2.1.2 Batimastat**

Batimastat ((4-(N-hydroxyamino)-2R-isobutyl-3S-(thienylthiomethyl)-succinyl)-L-phenylalanine-N-methylamide; mw = 478) was a kind gift from British Biotech (Oxford,

UK). Batimastat, a fine white powder, was prepared as a suspension of 3.0 mg/ml in phosphate buffered saline (PBS) containing 0.015% Tween-80 (pH 7.2). Tween-80 is a detergent which emulsifies batimastat, maintaining the compound in suspension. The suspension was prepared by vortexing for two minutes, followed by sonication for five minutes. This preparation was injected i.p. into mice at the dosage regimens indicated in the respective experiments. Stock suspensions of batimastat were kept at 4°C and discarded if not used within seven days.

### **2.1.3 Metastasis Assays**

Two experimental metastasis assays were performed (53), differing only in the dosage regimen of batimastat. Female C57Bl/6 mice (Harlan Sprague-Dawley, Indianapolis, IN) were used; this strain is syngeneic with B16F1 cells. Mice were anesthetized with 1.6 mg ketamine + 0.08 mg xylazine i.p. per 15 g body mass. The abdominal region was shaved and cleaned, and a small (~1.5 cm) longitudinal incision was made over the region of the cecum. The cecum was externalized, a large mesenteric vein was selected for injection, and  $10^5$  B16F1 cells in 0.2 ml of tissue culture medium with fetal calf serum was injected into the vein using a 30-gauge needle. The tip of the needle was bent at approximately 45° to facilitate the insertion of the needle into the vein. Before closing the wound, the peritoneal cavity was bathed with 1 ml sterile saline to counter dehydration. The abdominal wall incision was sutured with 5.0 silk thread, and the outer skin incision was closed with wound clips. The mice were kept warm throughout surgery and the recovery period with heat lamps. Mice were given analgesic upon waking and again 18 hours later (0.02-0.04 mg/kg Buprenorphine per dose). Batimastat was

administered in two regimens: Regimen 1: 30 mg/kg i.p. at 3, 8, 24, 48, and 72 hours post-injection (p.i.); Regimen 2: 50 mg/kg i.p. at -5 and +5 hours post-injection, and daily until the end of the experiment (21 total injections). Control animals received an equal volume of PBS + 0.015% Tween-80 (vehicle) i.p. at corresponding schedules. In regimen 1, six mice were used in each treatment group; in regimen 2, ten mice were used in each treatment group. At 19 days post-injection, mice were killed by CO<sub>2</sub> asphyxiation. Liver, lungs, kidneys, pancreas, spleen, stomach, intestines, and heart were removed and fixed in 10% formalin. The livers were weighed, and the number and diameter of liver tumors were determined using a dissecting microscope. All other extracted organs were examined for the presence of tumors.

#### **2.1.4 Data Analysis**

SigmaStat<sup>TM</sup> statistical software (Jandel Scientific, San Rafael, CA) was used for all statistical analyses. To determine if statistically significant differences existed between batimastat-treated and control groups, the student's t-test was used if the data had a normal distribution. If the distribution was not normal, the Mann-Whitney Rank Sum test was used. Parameters tested were mean liver tumor number, mean liver tumor size (diameter), the mean proportion of liver tumors less than two millimetres in diameter, and the mean proportion of liver tumors less than one millimetre in diameter.

## **2.2 Extravasation Assays**

### **2.2.1 Cell Culture and Fluorescent Labelling**

B16F1 cells were maintained in culture as described previously (section 2.1.1). In addition, a solution for fluorescently labelling the cells was prepared as follows (54): 375  $\mu$ l of stock 0.048  $\mu$ m diameter Fluoresbrite™ fluorescent carboxylate nanospheres (Polysciences Inc., Warrington, PA) was added to 50 ml OPTI-MEM minimal essential medium (GIBCO/BRL), and this solution was sterilized by passing through a 0.20  $\mu$ m filter. The filtered solution was allowed to sit overnight at 4°C, during which time the nanospheres settled to the bottom of the tube. OPTI-MEM (30 ml) was removed from the tube without disturbing the nanospheres. The nanospheres in the remaining 20 ml were vortexed into suspension and used to label cells.

Before harvesting for injection into mice, the tissue culture medium was removed from the flasks containing the cells, the cells were washed twice with OPTI-MEM, and 7.5 ml of the nanosphere solution was added to each flask. The cells were incubated for 90 minutes at 37°C to allow the cells to internalize the nanospheres, and following this incubation period the cells were washed three times with OPTI-MEM and harvested for injection into mice. Under epifluorescence illumination the labelled cells showed a green fluorescence. Before the injections, an average of 97.4% of cells excluded ethidium bromide for all injection series.

### **2.2.2 Extravasation Assay Preparation**

Three extravasation assays were performed, to determine the effects of batimastat on the extravasation of B16F1 cells from the mouse liver microcirculation at 8, 24, and 48

hours post-injection. (53, 54). Mouse surgery was performed exactly as it was for the experimental metastasis assays (section 2.1.3). For the extravasation assays,  $2 \times 10^5$  fluorescently labelled B16F1 cells were injected into a mesenteric vein for all experiments. Batimastat was administered at 50 mg/kg i.p. -5 and +5 hours post-injection, plus an additional dose at 24 hours for the 24 hour assay and at 24 and 48 hours for the 48 hour assay. Control animals received vehicle injections i.p. at corresponding schedules. For all three assays, four mice were used in each of the control and batimastat-treated groups.

To prepare for intravital videomicroscopy, mice were anesthetized with sodium pentobarbital (6 mg/kg i.p.) at 8, 24, or 48 hours post-injection. Two incisions were made along the abdomen: one along the midline, and one at an oblique angle to the midline to create a triangular flap of skin and abdominal wall. The mouse was placed on its side on an acrylic platform, and the liver was positioned so that the border of one lobe rested on a no. 1 coverslip mounted on the platform. Thread was tied around one point of the flap of skin, pulled back, and fastened to the platform to more fully expose the liver. Saran Wrap was used to cover the liver and prevent dehydration, and the temperature of the mouse was monitored using a rectal probe and maintained at 37° C with a heat lamp.

### **2.2.3 Intravital Videomicroscopy**

Intravital videomicroscopy was used to visualize cancer cells within the liver (51, 53, 54, and Figure 2.1). The acrylic platform with the mouse in position was placed on the stage of an inverted microscope (Nikon Diaphot TMD) equipped with objectives of magnifications X10, 20, 40, 60, and 100. Epifluorescence illumination (excitation wavelength 450-490 nm), oblique fiber-optic transillumination, or a combination of both,

were used to view the microcirculation. The epifluorescence illumination allows one to see the green fluorescent labelling of the cancer cells, and to determine the shape of the cells. Oblique fiber-optic transillumination allows one to view the liver microcirculation, to see blood cells flowing in sinusoids between surrounding hepatocytes, and the positions of the cancer cells with respect to these structures. The oblique lighting gave a shadowed, three-dimensional effect to the microcirculation, which enhanced depth perception. The microscope allowed "optical slicing" through the tissue by focusing up and down. Clear images of the liver microcirculation could be obtained as deep as 30  $\mu\text{m}$  below the liver surface.

Observations were made either through the eyepieces of the microscope or from a television monitor (Panasonic WV5410), which displayed images received from a black and white video camera (Panasonic WV1550) connected to the microscope. A character generator (Panasonic WJ810) added stopwatch information to the video image. Images were recorded on SVHS videotapes using a video cassette recorder (Panasonic AG7350), and black and white photographs of exceptional views within the microcirculation were taken directly from the video monitor using a 35 mm camera (Nikon F601).

Cancer cell position was divided into three categories with respect to the liver sinusoids: cells could be intravascular, in the process of extravasating, or extravascular. To distinguish cell position, established general criteria based on visual inspection of blood flow was used (53, 54): Intravascular cells appeared to completely block blood flow within microvessels; no red blood cells could pass by the cancer cell, and the cell had no visible extensions outside the vessel. Cells in the process of extravasating allowed blood cells to pass, but the flow was much slower than in surrounding vessels as the erythrocytes

had to squeeze past the cancer cell. These cells often had visible extensions into the surrounding hepatocyte layer. Extravasated cells did not visibly slow blood flow at all. Usually these cells appeared to be completely amongst the hepatocytes, but due to the three-dimensional nature of these observations extravasated cells located directly above or below vessels may have superficially appeared to be within the vessel. In these cases, normal flow within the vessel compared to surrounding vessels indicated an extravasated cell. A second researcher, Eric Schmidt, examined a sample of this visual data and confirmed the positions of the cancer cells. Following data collection, mice were killed by CO<sub>2</sub> asphyxiation.

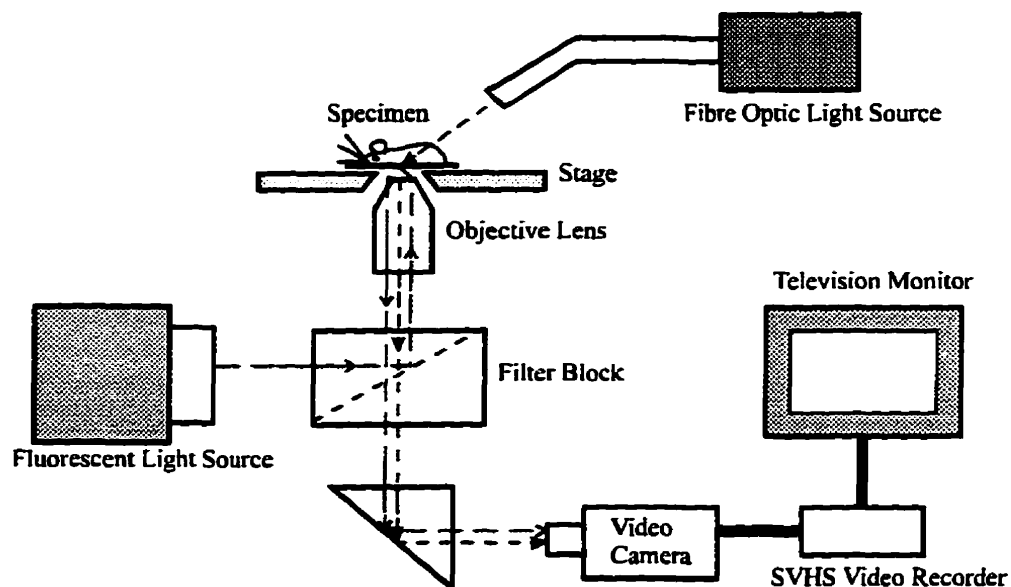


**Figure 2.1** Schematic of intravital videomicroscopy (IVVM). The mouse is placed on the stage of an inverted microscope with the organ of choice exposed (in these studies it is the liver). Oblique transillumination and episcopic fluorescence are used to view the liver microcirculation. Images can be captured by a video camera and sent to a television monitor and SVHS VCR.

#### **2.2.4 Data Analysis**

To assess statistical significance, the student's t-test was used if the data had a normal distribution. If the distribution was not normal, the Mann-Whitney Rank Sum test was used. Sample sizes were the number of mice, not the number of cells. These tests were used to determine if significant differences existed between batimastat-treated and control groups in terms of cell position (intravascular, in the process of extravasating, and extravascular) at each time point (8, 24, and 48 hours).

### **2.3 Initial Growth Assay**

#### **2.3.1 Cell Culture and Microsphere Addition**

B16F1 cells were maintained in culture as mentioned previously. Prior to injection into mice, cells were fluorescently labelled with Fluoresbrite™ carboxylate nanospheres using the same protocol as for the extravasation assays (section 2.2.1). Following harvest of the cells, 10.2 µm inert polystyrene microspheres (Bangs Laboratories, Fisher, IN) were added to the cells such that the cell-to-microsphere ratio was approximately 10:1. Before each injection, the exact ratio of cells to microspheres in the syringe was determined with a Nikon Diaphot TMD inverted microscope, using epifluorescence to identify cells and oblique transillumination to identify microspheres. When injected into the portal circulation, all 10.2 µm microspheres become lodged in the liver microcirculation. By injecting a known ratio of cells to microspheres, the microspheres were used as a standard to measure cell survival in the liver. Our group has used this microsphere technique to measure cell survival in the chick chorioallantoic membrane (55). Prior to injection, 96.1% of cells excluded ethidium bromide.

### **2.3.2 Surgery and Batimastat Administration**

Mouse surgery was performed as in the experimental metastasis assays. Cell-microsphere mixtures containing  $2 \times 10^5$  cells were injected into each mouse via a mesenteric vein. Batimastat was administered at 50 mg/kg i.p. -5 and +5 hours post-injection and daily until the end of the experiment at four days. Control animals received vehicle injections at corresponding schedules. Six mice were used in each treatment group. At four days post-injection, mice were killed by CO<sub>2</sub> asphyxiation, and the livers were removed and fixed in 10% formalin.

### **2.3.3 Liver Sectioning**

Following formalin fixation for a minimum of 24 hours, sections were cut from each liver using a Vibratome Series 1000<sup>TM</sup> sectioning system (Technical Laboratories International, St. Louis, MO). For each liver, a lobe was cut off and fixed to a small block using Superglue<sup>TM</sup>. The block was placed in the Vibratome, and lobe, block, and sectioning blade were completely immersed in ice and 0.9% saline. Eight to ten 30  $\mu$ m thick sections of the liver lobe were cut. These sections were placed on 40 x 22 mm slides, petroleum jelly was sparingly spread around the perimeter of the sections to provide an airtight seal, and small coverslips were placed on top of the sections.

### **2.3.4 Growth Assay**

A Nikon Diaphot TMD inverted microscope was used to examine the liver sections. Using fluorescence illumination only at 40X magnification, single cancer cells could be easily distinguished within the sections. Micrometastases could be easily

identified, too, by their distinctive black melanin against the faint green background created by weak fluorescence of the formalin. Microspheres were identified using oblique transillumination only, and could easily be seen due to their refractive index being different from that of the liver tissue.

### **2.3.5 Data Analysis**

The number of cells, microspheres, and micrometastases per section were tallied until four sections or 60 microspheres were counted per liver, whichever came first. Micrometastasis-to-single cell ratios were calculated for each liver; these ratios were representative of the rate of initial growth of single cells into micrometastases. Cell-to-microsphere ratios were calculated to quantify cell survival. The student's t-test or the Mann-Whitney Rank Sum test was used to determine if differences in either ratio existed between batimastat-treated and control groups. Sample sizes were the number of mice, not the number of cells.

## **2.4 Tumor Angiogenesis Assay**

### **2.4.1 Tissue Fixation and Embedding**

Livers from mice used in the experimental metastasis assay, treatment regimen 2, were used here. Liver tissue was fixed in 10% formalin overnight following removal from the animal. Tumors of varying sizes (1, 2, and 3 mm diameter) were excised with a scalpel from both batimastat-treated and control livers. Care was taken to excise the entire tumor and include some of the surrounding liver tissue. Samples of control liver and lung tissue

were also excised. Each sample was placed in an embedding cassette and embedded in paraffin.

#### **2.4.2 Tissue Staining**

The excised and embedded tissue was stained with hematoxylin and eosin (H&E). These procedures were kindly carried out by Ms. Nancy Kerkvliet. Tissue sections were cut to 4  $\mu\text{m}$  thickness and mounted on positively charged adhesive slides. The tissue was deparaffinized with xylene, and cleared of xylene with 100% ethanol. Sections were hydrated sequentially with 95% ethanol, 80% ethanol, 70% ethanol, and distilled water. The tissue was stained with Harris' Hematoxylin for 4 minutes. The sections were rinsed with running tap water, followed by a rinse in distilled water. The tissue was treated with 1% acid alcohol for 5-10 seconds, followed by rinses in running tap water and distilled water. The slides were placed in 80% alcohol for 1 minute, and stained in eosin for 3 minutes. The tissue was dehydrated with three changes of isopropyl alcohol and rinsed with three changes of xylene. The slides were then covered with permanent mounting media.

#### **2.4.3 Angiogenesis Assay**

The extent of angiogenesis within tumors was determined using a novel technique developed in our lab. H&E stained sections were observed using an inverted microscope (Nikon Diaphot TMD). Illumination was provided by a fibre optic light source fixed directly above the microscope stage; this lighting allowed red blood cells to be clearly visible within vessels even at low (10X) magnification. Tumor tissue stained darkly and

was readily identifiable in contrast to the surrounding normal liver tissue which stained light pink with purple nuclei. Red blood cells were visible in tumor and liver tissue, and were used to identify the presence of blood vessels.

Colour photographs were taken of ten tissue sections, each containing one liver tumor, using a 35 mm camera (Nikon F601) attached to the microscope. The ten tumors photographed included five from batimastat-treated mice and five from control mice: each group of five included two ~ 1 mm (diameter) tumors, two ~ 2 mm tumors, and one ~ 3 mm tumor. All photographs were taken using a 10X objective lens. In cases where more than one photograph was required to record the entire tumor, the photographs were assembled into a composite image of the tumor.

Vessel density within the tumors was measured stereologically by placing an acetate sheet containing a square grid of lines over each photograph and counting the number of points on the grid that fell on red blood cells within the tumor. Any uncertainty regarding the identification of red blood cells was resolved by examining the original section under higher magnification using the microscope. Two of the photograph composites of batimastat-treated tumors contained large pools of erythrocytes. These areas were interpreted as hemorrhage and were not scored as vessels. The number of points falling on red blood cells within a tumor was divided by the total number of grid points that fell on the tumor. The resulting values represented the point density ( $P_p$ ) of blood vessels within the tumor, which is the stereological equivalent of  $V_v$ , the volume density of blood vessels within the tumor. Thus, these measured values of  $P_p$  were representative of the fraction of the tumor volume occupied by blood vessels, which was a good indication of the degree of angiogenesis. The diameter of each tumor was also

measured from the photographs. These values showed good correlation with the gross measurements of tumor diameter taken when removing the tumors for sectioning: seven of ten measurements from photographs were slightly less than the gross measurements, and three of ten were slightly more. Gross measurements of tumor diameter were used for data analysis, as it was not certain whether the photographs represented sections taken from the centre of the tumors and thus the photographs may not have represented the true diameter of the tumors.

#### **2.4.4 Data Analysis**

The mean vessel density (as measured by  $V_v$ ) was calculated for each tumor diameter category (one, two, and three millimetres) separately for both treatment groups. The paired t-test was used to determine if a significant difference existed between treatment groups in terms of mean vessel density at each diameter category. In other words, the differences between treatment groups were determined for each diameter category, and the mean of these three values of differences was tested to determine if it was significantly different from zero. A paired t-test was used instead of the student's t-test in order to exclude inherent variation in vascular density between tumors of different sizes.

## Chapter 3: Results

### 3.1 Experimental Metastasis Assays

Tables 3.1 and 3.2 show the results of the two experimental metastasis assays performed to test the effectiveness of batimastat in reducing metastasis to the mouse liver following B16F1 cell injection. When batimastat was administered at 30 mg/kg i.p. 3, 8, 24, 48, and 72 hours post-injection (regimen 1), the mean number of liver tumors and the mean tumor diameter at 19 days post-injection were not reduced compared to controls (Table 3.1). In addition, the proportion of tumors 2 mm in diameter or less and the proportion 1 mm in diameter or less were likewise not affected by batimastat. This latter data was included because any differences noted may indicate an effect of batimastat on angiogenesis, as this process is required for tumors to exceed 1-2 millimetres in diameter. There were no apparent differences between the treatment groups in the distribution of tumors throughout the rest of the tissues. Common sites for nodule growth included the small and large intestine, the mesenteric tissue, and the thoracic lymph ducts.

When batimastat was administered at 50 mg/kg i.p. -5, +5 hours post-injection and daily until the end of the experiment at day 19 (regimen 2, 21 total doses), it caused a 23.1% reduction in the mean liver tumor diameter ( $P = 0.011$ ), with no effect on tumor number (Table 3.2). The batimastat-treated group also displayed a 53.2% increase in the proportion of liver tumors 2 mm or less in diameter compared to controls ( $P = 0.0038$ ) and a 78.5% increase in the proportion of liver tumors 1 mm or less in diameter compared to controls ( $P = 0.048$ ). There were no apparent differences between treatment groups in

the distribution of nonhepatic tumors, and the common sites for these tumors were the same as with regimen 1.

All of the mice which received batimastat in regimen 2 displayed white clumps of batimastat in the abdominal cavity upon post-mortem examination; conversely, none of the mice which received batimastat in regimen 1 had any white residue in the abdominal cavity. This indicates that much of the batimastat given in regimen 2 was not absorbed into the system, and suggests that the increase in per dose amount from 30 mg/kg in regimen 1 to 50 mg/kg in regimen 2 was not a significant factor affecting the results. All of the mice which received batimastat in regimen 2 displayed blood in the peritoneal cavity, while all of the mice which received batimastat in regimen 1 and all control mice from both experiments had no blood in the peritoneal cavity.

**Table 3.1** 19-day experimental metastasis assay to test the ability of batimastat, regimen 1, to reduce metastasis to the liver. Batimastat was administered at 30 mg/kg i.p. 3, 8, 24, 48, and 72 hours following B16F1 cell injection.

Treatment	n	Mean Number of Liver Tumors <sup>a</sup>	Mean Tumor Diameter (mm) <sup>b</sup>	Tumors ≤ 2mm diameter (%) <sup>c</sup>	Tumors ≤ 1mm diameter (%) <sup>d</sup>
Batimastat	6	29.3±9.2	3.67±0.47	41.8±9.5	11.1±7.0
Control	6	18.7±6.2	3.61±1.15	40.7±16.2	10.9±11.6

<sup>a</sup>P = 0.041; <sup>b</sup>P = 0.908; <sup>c</sup>P = 0.887; <sup>d</sup>P = 0.966

**Table 3.2** 19-day experimental metastasis assay to test the ability of batimastat, regimen 2, to reduce metastasis to the liver. Batimastat was administered at 50 mg/kg i.p. -5, +5 hours and daily thereafter following B16F1 cell injection.

Treatment	n	Mean Number of Liver Tumors <sup>a</sup>	Mean Tumor Diameter (mm) <sup>b</sup>	Tumors ≤ 2mm diameter (%) <sup>c</sup>	Tumors ≤ 1mm diameter (%) <sup>d</sup>
Batimastat	10	55.5±21.8	2.47±0.42	65.1±14.0	26.6±14.1
Control	10	58.8±19.1	3.21±0.72	42.5±16.4	14.9±10.5

<sup>a</sup>P = 0.723; <sup>b</sup>P = 0.011; <sup>c</sup>P = 0.0038; <sup>d</sup>P = 0.048

### **3.2 Extravasation Assays**

Figure 3.1(a-c) shows the results of the 8, 24, and 48 hour assays to test the ability of batimastat to inhibit the extravasation of B16F1 cells from the liver microcirculation. Batimastat was administered at -5 and +5 hours post-injection and then every 24 hours until the end of the respective assay. The results are represented as the percentage of cells at each time point which are intravascular, in the process of extravasating, or wholly extravascular. At all three time points, there were no significant differences between the batimastat and control groups at any of the three cell positions (P-values ranged from 0.343 to 0.963). This indicates that batimastat did not have an inhibitory effect on B16F1 cell extravasation. Photographs of an intravascular B16F1 cell, a cell in the process of extravasation, and an extravascular cell within the liver parenchyma are displayed in Figure 3.2(a-c). These photographs are taken directly from the television monitor, and serve as a good illustration of the high quality images that can be obtained with IVVM.

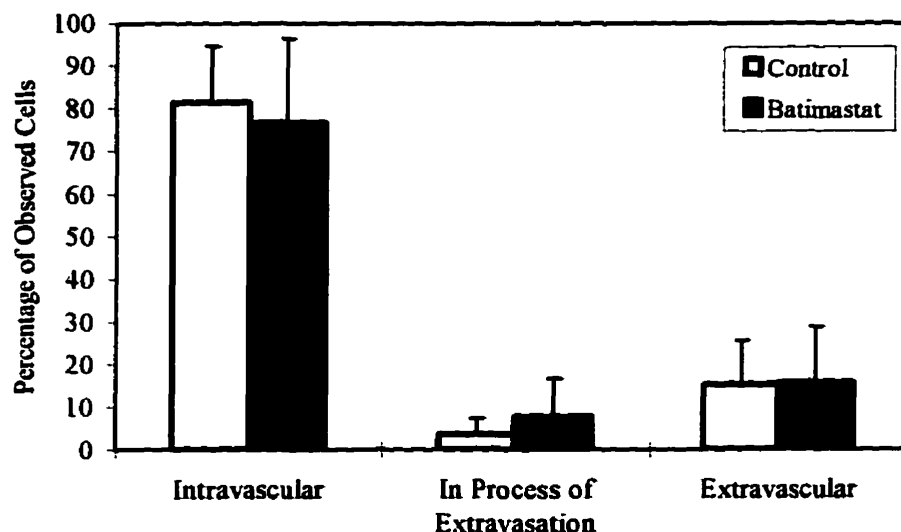


**Figure 3.1(a)** 8 hour IVVM extravasation assay. Batimastat was administered at 50 mg/kg -5 and +5 hours after B16F1 cell injection. Livers of mice were viewed 7-9 hours p.i. Number of mice: 8; number of cells: 319. There were no significant differences between the batimastat group and the control group at any cell position ( $P > 0.05$ ).

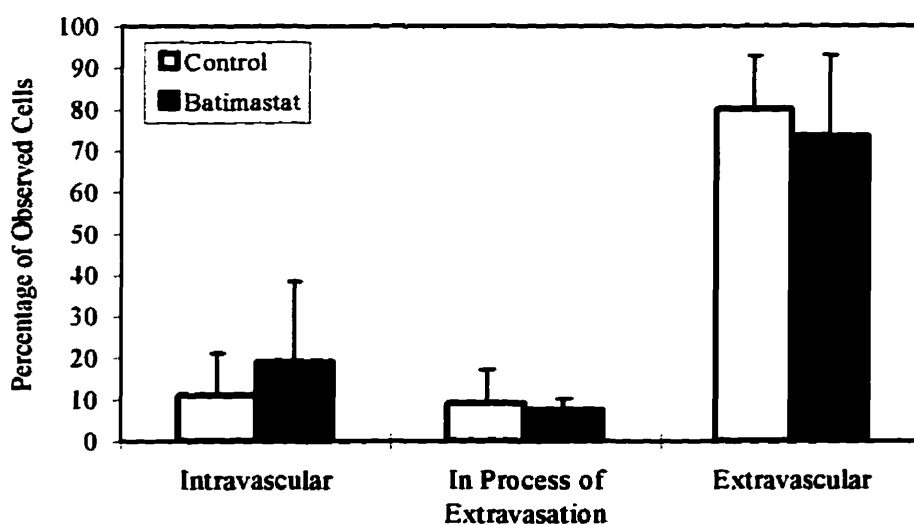


**Figure 3.1(b)** 24 hour IVVM extravasation assay. Batimastat was administered at 50 mg/kg -5, +5, and +24 hours after B16F1 cell injection. Livers were viewed 24-28 hours p.i. Number of mice: 8; number of cells: 296. There were no significant differences between the batimastat group and the control group at any cell position ( $P > 0.05$ ).

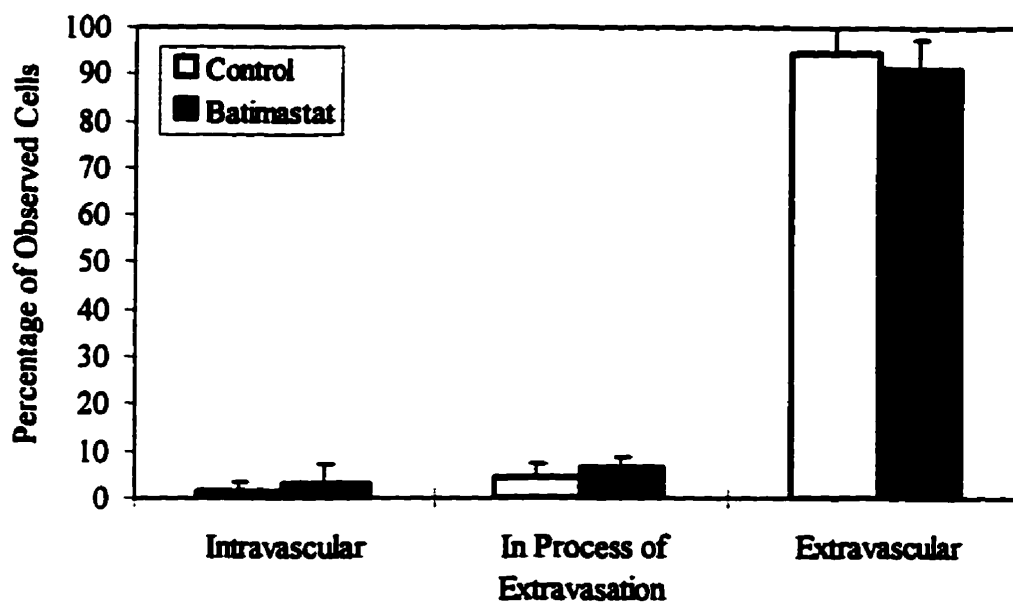


**Figure 3.1(c)** 48 hour IVVM extravasation assay. Batimastat was administered at 50 mg/kg -5, +5, +24, and +48 hours after B16F1 cell injection. Livers were viewed 48-51 hours p.i. Number of mice: 8; number of cells: 385. There were no significant differences between the batimastat group and the control group at any cell position ( $P > 0.05$ ).

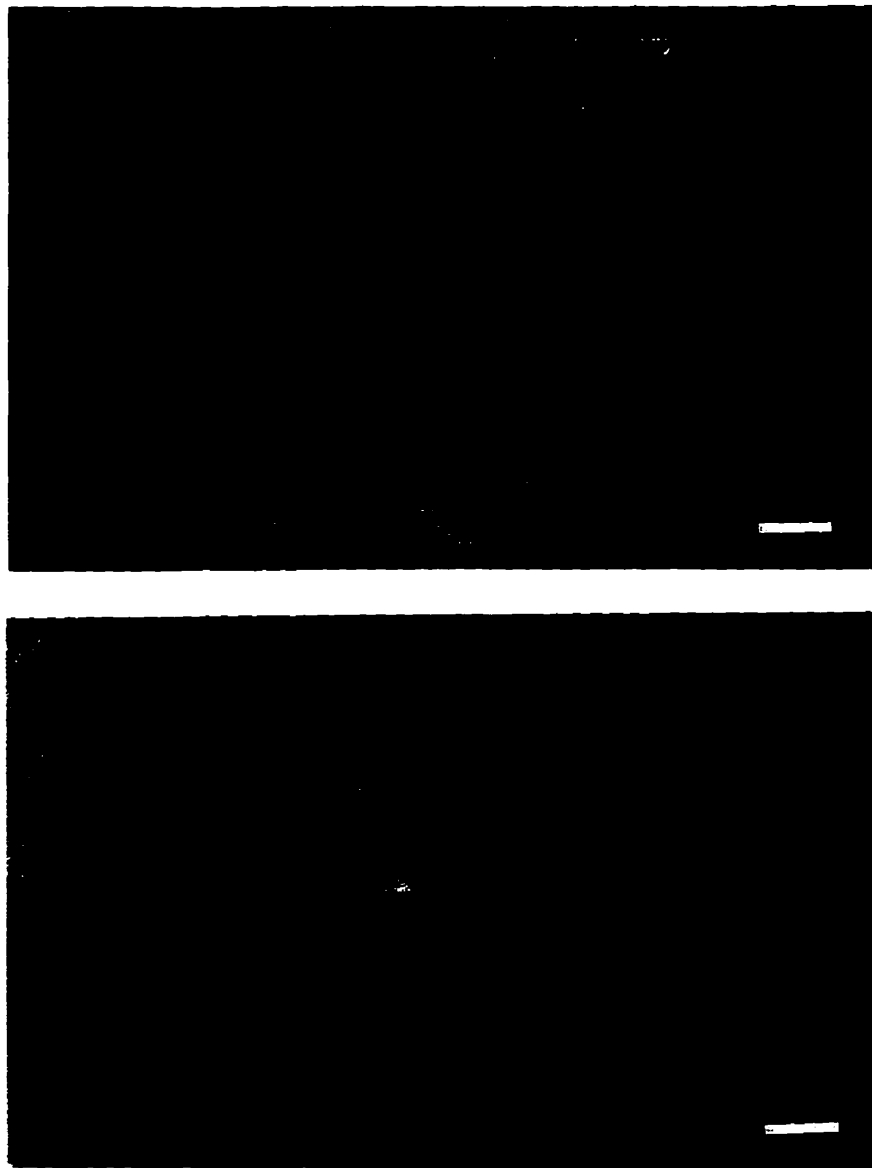
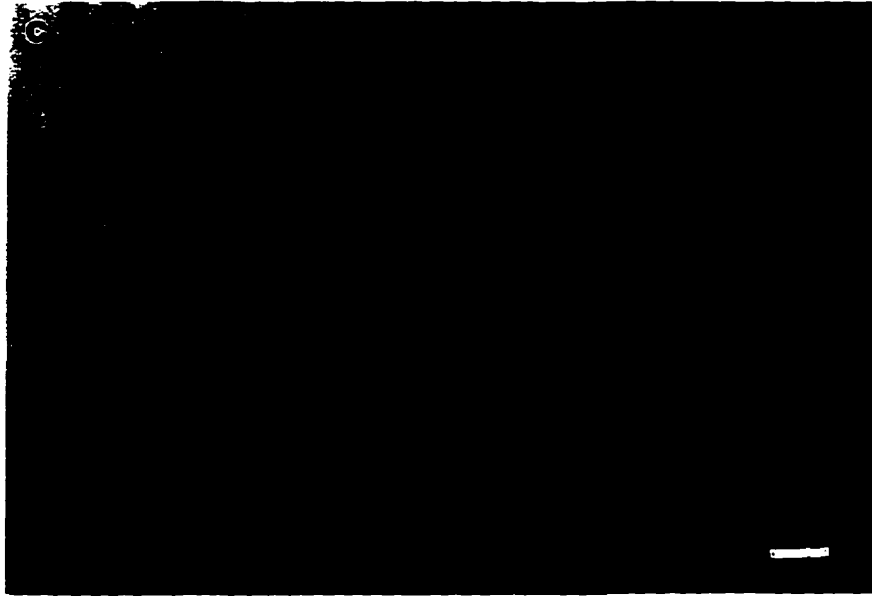


**Figure 3.2** IVVM images of cells in the liver microcirculation.

**(a)** An intravascular B16F1 cell. This cell (→), visible by its melanin content, is completely within a liver sinusoid (S). The flow of blood was stopped by this cell; stationary red blood cells can be seen. H: hepatocytes; bar = 10  $\mu\text{m}$ .

**(b)** A B16F1 cell in the process of extravasation. This cell (→) is clearly visible by its fluorescence (white spot). It has nearly finished extravasating from a liver sinusoid (S) into the surrounding hepatocytes (H). Note the red blood cells forced to squeeze past it: this indicates that the cell is still partially within the sinusoid lumen. Bar = 10  $\mu\text{m}$ .



**(c)** Two extravasated B16F1 cells. These cells (→) have completely exited a sinusoid (S) and are amongst the surrounding hepatocytes (H). The lower cell appears to protrude into the vessel, but optical slicing with the microscope revealed that the vessel is completely beneath the cell. Visible streaks within the sinusoid indicate red blood cells flowing normally. Bar = 10  $\mu\text{m}$ .

### **3.3 Initial Growth Assay**

Subsequent to the discovery that batimastat did not inhibit extravasation, this compound was tested for its ability to prevent the initial growth of single cancer cells into micrometastases by four days following the injection of B16F1 cells. Table 3.3 summarizes the results of this initial growth assay. Batimastat did not inhibit the initial growth of micrometastases; instead, the mean rate of occurrence of micrometastases in livers from batimastat-treated mice was more than three times that observed in controls (38.9/1000 cells vs 12.0/1000 cells;  $P = 0.041$ ).

Batimastat did not have an effect on the survival of single cells in the liver (Table 3.3). Cell survival for each liver was calculated by dividing the single cell-to-microsphere ratio present in the sections by the single cell-to-microsphere ratio in the syringe prior to the initial injection of cells, and expressing this fraction as a percentage. The batimastat-treated livers displayed a lower mean cell survival than the control livers (72.1% vs 88.4%), but due to high variability, this difference was not significant ( $P = 0.319$ ). Images of a single cell and a microsphere in a liver section are displayed in Figure 3.3, and an image of a micrometastasis in a liver section is displayed in Figure 3.4.

**Table 3.3** Initial growth assay. Batimastat was administered at 50 mg/kg i.p. -5, +5, +24, +48, +72, and +96 hours following B16F1 cell injection. Livers were sectioned and assayed at four days post-injection.

Treatment	n	Mean Cell Survival (%) <sup>a,b</sup>	Mean # Micrometastases (per 1000 cells) <sup>c</sup>
Batimastat	6	72.1 ± 21.1	38.9 ± 40.8
Control	6	88.4 ± 31.7	12.0 ± 20.4

<sup>a</sup> Cell survival =  $\frac{\text{single cells/microspheres in sections}}{\text{single cells/microspheres in syringe}} \times 100\%$

<sup>b</sup> P = 0.319

<sup>c</sup> P = 0.041

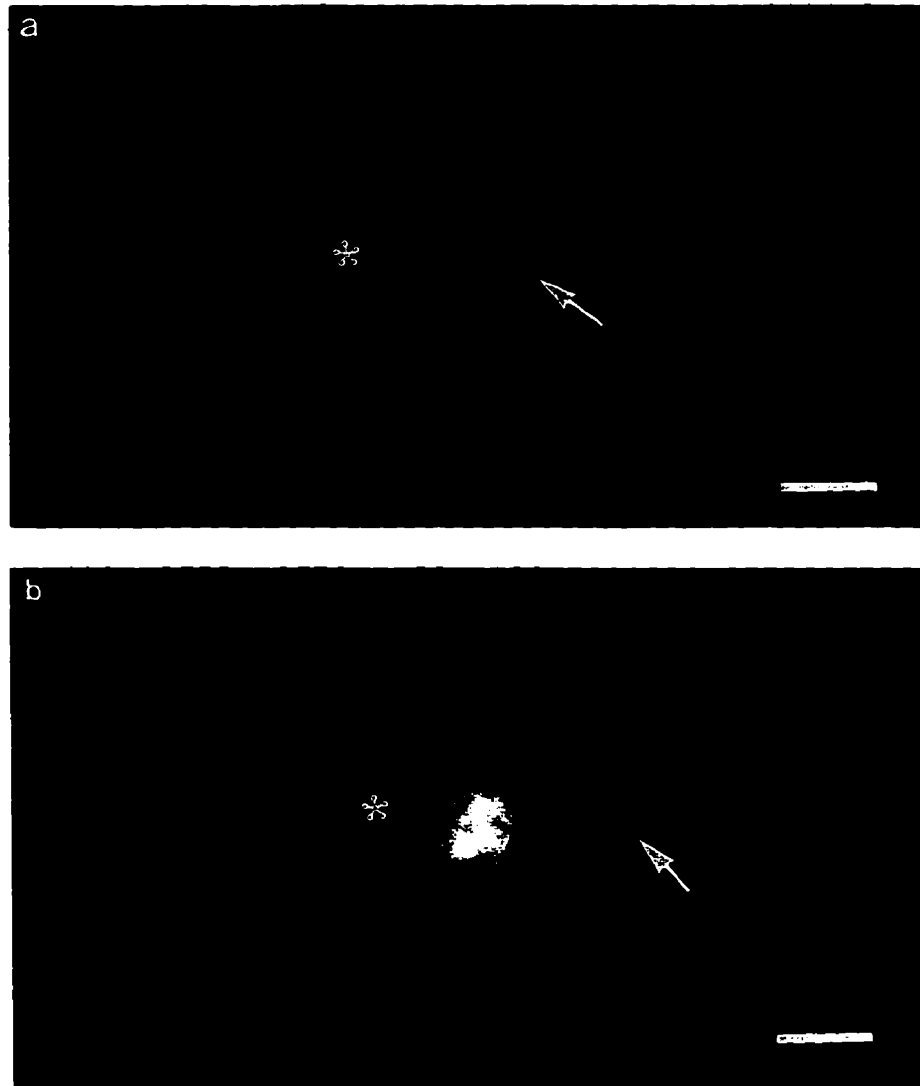


**Figure 3.3** A B16F1 cell and a 10.2 μm microsphere in a 30 μm section of mouse liver tissue at 4 days p.i.

**(a)** View of the B16F1 cell and the microsphere using fibre optic transillumination and fluorescence illumination. The fluorescently labelled cell (beside the \*) is readily visible against the red background. The microsphere (→) is easily seen due to its distinct refractive index. These illumination conditions were used to count microspheres. Bar = 20 μm.

**(b)** View of the B16F1 cell and the microsphere using fluorescence illumination only. The fluorescent image of the cell (beside the \*) is much more distinct than in the previous figure. The microsphere (→) is difficult to see; its presence could not be confirmed without using transillumination. These illumination conditions were used to count single cells and micrometastases. Bar = 20 μm.

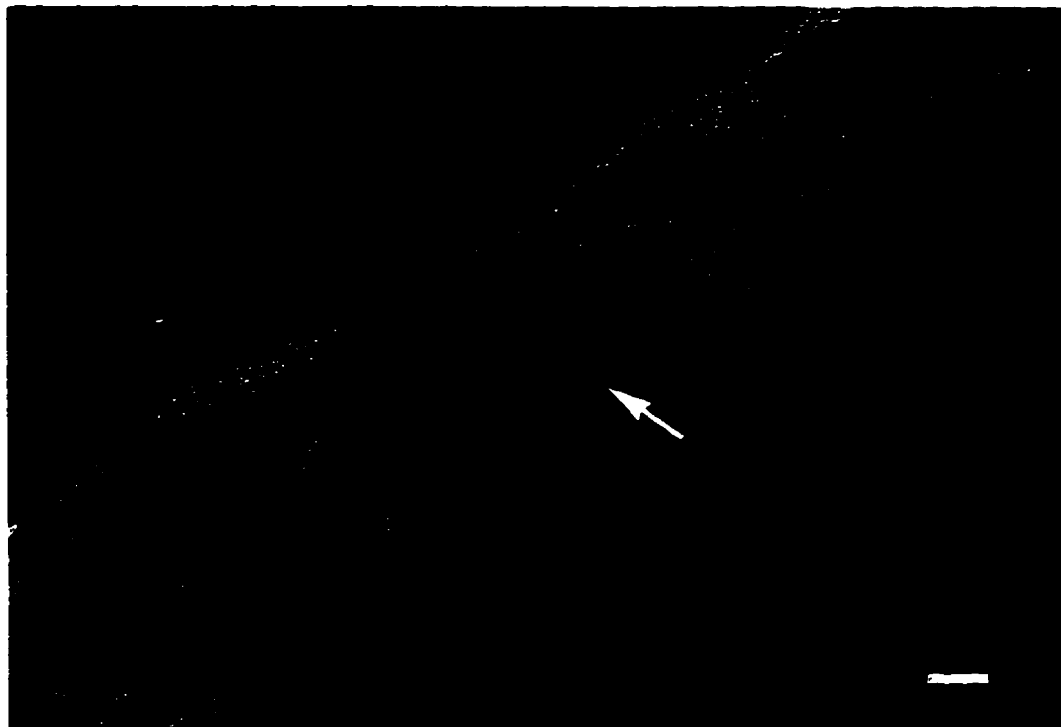


**Figure 3.4** A micrometastasis in a 30  $\mu\text{m}$  section of mouse liver tissue at 4 days p.i. Only fluorescence illumination is necessary to detect this melanotic micrometastasis ( $\rightarrow$ ) close to the edge of the tissue section. This photograph is a good illustration of the ease in detecting micrometastases within the liver sections. Bar = 20  $\mu\text{m}$ .

### **3.4 Angiogenesis Assay**

To complete this study, batimastat was tested for its ability to inhibit the final major stage of the metastatic process: angiogenesis within metastatic tumors. This was done by placing a grid on photographs of H&E stained sections of 19-day liver tumors (Figure 3.6) and scoring the proportion of grid points that fell on red blood cells. This proportion represented the stereological value of  $V_v$ , or the fraction of the volume of the tumor occupied by blood vessels. Figure 3.5 displays the results of this comparison of tumor vascular density between batimastat-treated and control groups. It is visually apparent that, for all three tumor diameter categories (one, two, and three millimetres), the vascular density of tumors from the batimastat-treated group is considerably lower than the vascular density of control tumors. However, due to the small sample size, statistical analysis of these differences was crucial to support this observation. A paired t-test showed that the mean difference in vessel density within each of the three tumor diameter categories was significantly different from zero ( $P = 0.011$ ). I conclude that treatment with batimastat caused a reduction in the vascular density of 19-day liver tumors compared to controls.

Upon qualitatively examining the photograph composites, striking differences between the batimastat-treated and control groups were noted. The three smallest control tumors were well vascularized throughout with vessels of varying size (Figures 3.6, 3.7(a)). The cells of these three tumors appeared healthy in all areas. The two largest control tumors appeared to have lesser vessel densities, with patches of scattered necrotic tissue. Large vessels were quite apparent throughout the largest control tumor. In

general, there were no tumor regions (i.e. periphery, centre) which appeared to have greater vascular density than others.

The five batimastat treated tumors each appeared to have lowered vascular density compared to control tumors of the same size. The cells of the three smallest treated tumors did not appear as distinct and healthy as the those of the three smallest control tumors. In two of the three smallest treated tumors, there was a large blood-filled space in the centre which was interpreted as hemorrhage (Figure 3.7(b)). In the two largest treated tumors, there was a complete absence of large vessels; only a few small scattered vessels were apparent. Similar to the control tumors, there did not appear to be any regions of universally increased or decreased vascularity within the batimastat treated tumors, although a few individual treated tumors displayed regions of varying vascular density.

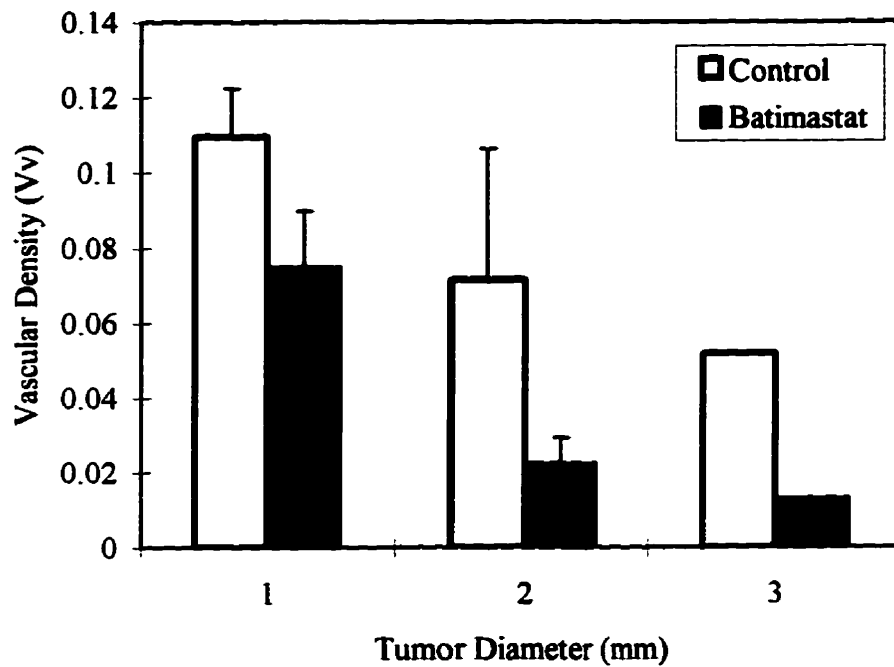


**Figure 3.5** Vascular density in liver tumors of varying diameter. The liver tumors are from the 19-day experimental metastasis assay in which batimastat was administered in regimen 2. The vascular density is expressed as  $V_v$ , the fraction of tumor volume occupied by blood vessels. Batimastat treatment resulted in a significant reduction of vascular density compared to controls ( $P = 0.011$ ). For tumors of 1 and 2 mm diameter,  $n = 2$  for both treatment groups. For 3 mm tumors,  $n = 1$  for both treatment groups, and therefore no error bars are present.

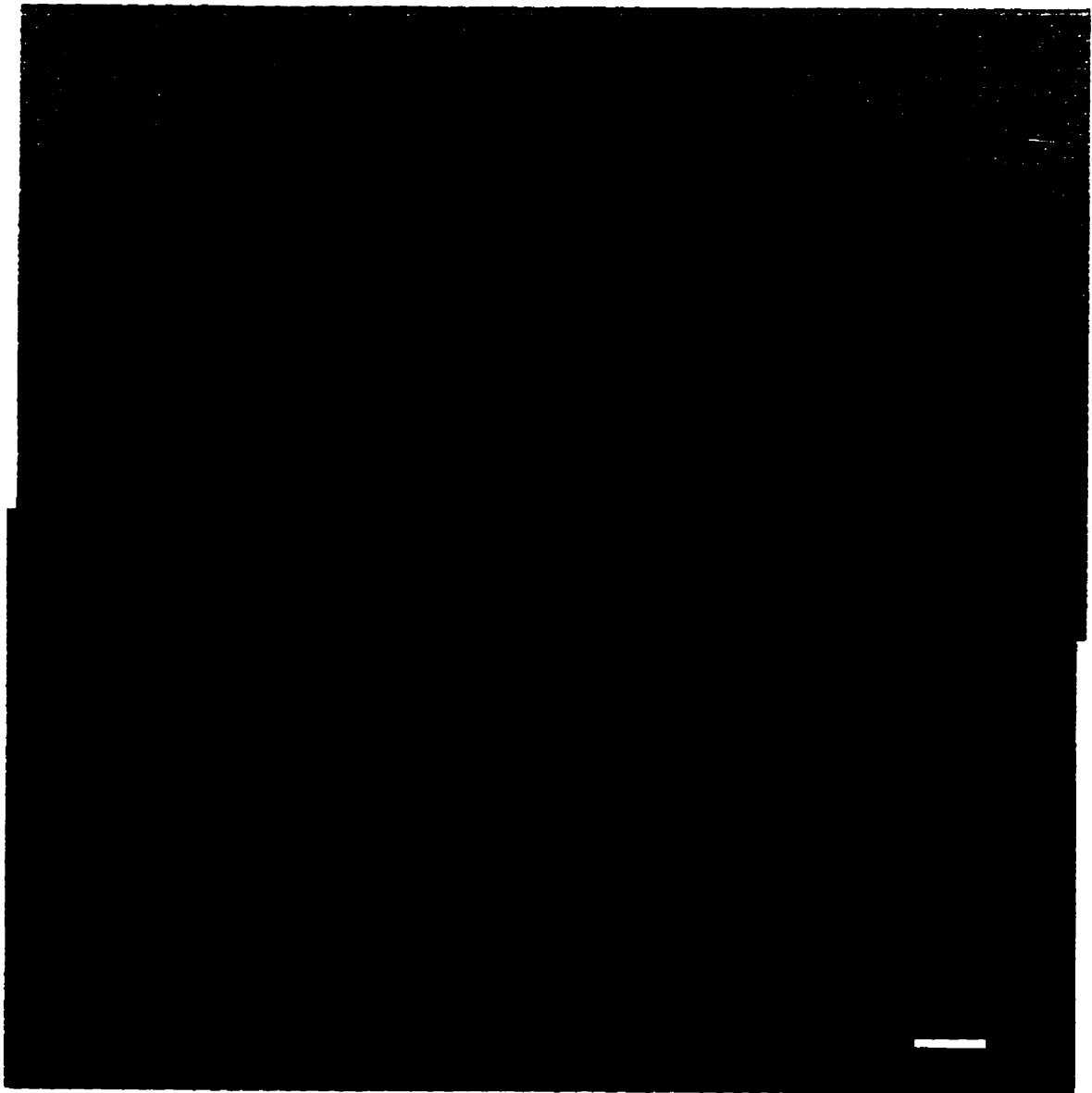


**Figure 3.6** A composite image of a one millimetre liver tumor from the control group at 19 days p.i. This composite image was constructed from two overlapping photographs of H&E stained liver tissue sections viewed with the 10X objective. The darkly stained cells comprise the tumor, while the lighter, pink cells represent normal liver tissue. A definite border separating these tissues can be seen. The distinct red appearance of erythrocytes illustrates the presence of blood vessels. Composite images such as these were used to determine the vessel density within tumors. Bar = 100  $\mu$ m.

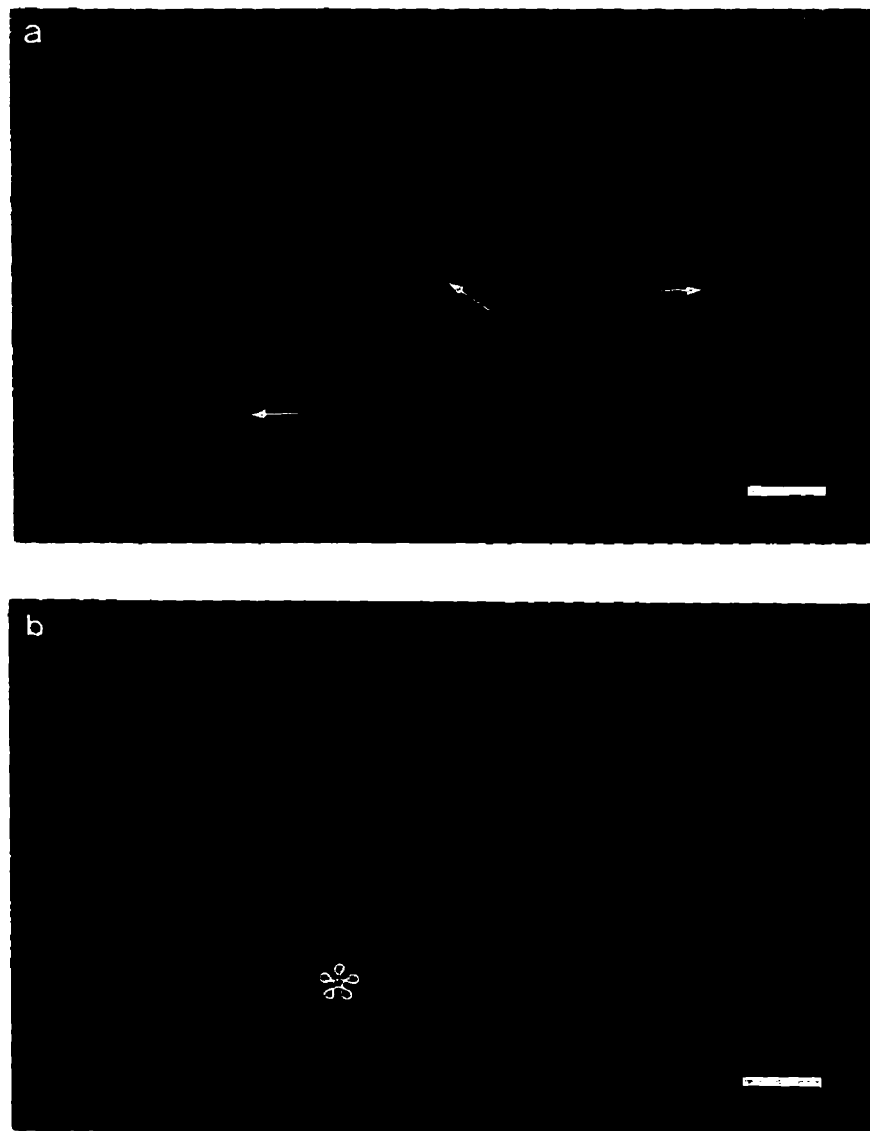


**Figure 3.7** Interior of two 1-millimetre tumors at 19 days p.i.: one from the control group and one from the batimastat-treated group. These photographs were taken of images using the 20X objective.

**(a)** Interior of a 1-millimetre control tumor. The cells contain distinct nuclei, and clear borders exist between cells. Vessels containing red blood cells ( $\rightarrow$ ) are abundant (not all vessels are indicated by arrows). Bar = 50  $\mu\text{m}$ .

**(b)** Interior of a 1-millimetre batimastat-treated tumor. Nuclei within the cells are less distinct, as are the borders between cells. A large blood-filled space (\*) occupies a large portion of this image. It is likely that the empty space to the top right of the blood-filled space would soon have filled with blood. Bar = 50  $\mu\text{m}$ .

## **Chapter 4: Discussion and Conclusions**

These studies represent the first time that anyone has examined extravasation, the initial growth of micrometastases, and angiogenesis in an attempt to determine more precisely the mechanisms of action of an anticancer drug. Prior to this, drug testing consisted mainly of metastasis assays in which cancer cells are injected, the drug is administered, and the tumors are assayed a certain time later. A “black box” existed between the beginning and end results of these assays; there was only speculation on which steps of metastasis were affected.

### **4.1 Metastasis to the Mouse Liver**

Matrix metalloproteinases have long been implicated in facilitating cancer metastasis (19). The synthetic matrix metalloproteinase inhibitor batimastat has previously been shown to reduce experimental hematogenous metastasis to the lung in mice (40-42), as well as experimental metastasis to the liver (41: intraperitoneal injection of cells, i.e. not a hematogenous metastasis assay). I have shown, for the first time, that batimastat is able to reduce experimental hematogenous metastasis to the liver in mice: administration of batimastat at 50 mg/kg i.p. five hours before and after B16F1 melanoma cell injection and daily until the end of the experiment at day 19 (regimen 2), resulted in a 23.1% reduction in the mean diameter of liver tumors, a 53.2% increase in the proportion of tumors two millimetres in diameter or less, and 78.5% increase in the proportion of tumors one millimetre in diameter or less. All three differences were significant ( $P < 0.05$ ). There

were no differences in the mean number of liver tumors between the batimastat-treated and control groups.

Batimastat was not able to reduce the mean number of liver tumors, the mean tumor size, or the mean proportion of tumors one or two millimetres in diameter or less when the drug was administered at 30 mg/kg i.p., at 3, 8, 24, 48, and 72 hours following B16F1 cell injection (regimen 1). To account for the differences in treatment outcomes between the two regimens, the two major differences between the regimens were considered: single dose amount and timing of doses. The differing effects are not likely due to a higher single dose amount (50 mg/kg vs 30 mg/kg), as the excess batimastat observed in the abdomen of mice who received 50 mg/kg indicate that a lower dose such as 30 mg/kg would likely have resulted in similar levels of drug in the circulation. However, it may have been necessary to maintain a certain level of batimastat in the circulation for the duration of the experiment in order to achieve inhibition of metastasis. Regimen 2, consisting of daily doses of batimastat, likely maintained a level of the drug in the circulation throughout the experiment, while regimen 1, consisting of doses only during the first 72 hours, did not maintain a level of batimastat in the circulation. Thus, it appears likely that the reduction in liver tumor sizes observed with regimen 2 but not with regimen 1 was due to the daily administration of batimastat throughout the 19-day experiment.

It is interesting that, with treatment regimen 1, the batimastat-treated group had a significantly higher number of liver tumors than the control group (29.3 vs 18.7, respectively,  $P = 0.041$ ). Batimastat treatment during the first 72 hours post-injection may have presented a challenge to the cells, which caused a greater proportion of single cells to

begin growing once batimastat treatment ceased, resulting in more liver tumors. However, with a sample size of only six and a P-value very close to 0.05, this stimulatory effect on tumor number should be interpreted with caution; it is within reason that this observed difference is merely due to chance variation.

The clinical significance of the observation that batimastat reduces metastasis to the liver should be addressed. Our model is an experimental hematogenous metastasis assay, in which a bolus of cancer cells is injected directly into the blood circulation. An experimental hematogenous metastasis assay does not perfectly mimic the clinical situation, where an antimetastatic drug must be able to inhibit the formation or growth of secondary tumors arising from an existing or excised primary tumor. Cancer cells grown in culture may differ significantly from those that are shed from a primary tumor *in vivo* in terms of the expression of various factors, such as proteases, that will enable them to complete the metastatic process. In addition, a hematogenous metastasis assay involves only the blood circulation, and thus does not test the ability of the compound to inhibit metastasis via the lymphatics or body cavities. Nevertheless, batimastat has been shown to inhibit spontaneous metastasis and metastasis through a body cavity. Wang et al. (39) demonstrated that, of 38 nude mice bearing a primary human colon carcinoma tumor, only 2 of 20 batimastat-treated mice displayed distant metastatic tumors, compared to 6 of 18 control mice which displayed distant metastases. Also, Watson et al. (41) discovered that batimastat treatment reduced the number of liver tumors by 65% and the size of liver tumors by 57% compared to controls, following the injection of C170HM<sub>2</sub> human colorectal cancer cells into the peritoneal cavity of nude mice. Thus, although our model does not perfectly mimic the clinical situation, batimastat has been shown to be effective in

inhibiting the aspects of metastasis which experimental hematogenous metastasis assays do not address.

## **4.2 Extravasation from Liver Sinusoids**

Since batimastat demonstrated ability in reducing metastasis to the liver in an experimental hematogenous metastasis assay, the stage or stages of the metastatic process inhibited by this compound were investigated. We initially hypothesized that batimastat inhibited extravasation, as this is the first challenge faced by the cancer cell following its arrest in the microcirculation, and has long been considered to be a major barrier to the metastatic process (48). Using intravital videomicroscopy, we investigated the effects of batimastat on the extravasation of B16F1 melanoma cells from liver sinusoids by examining the position of the cancer cells relative to the sinusoids at 8, 24, and 48 hours following injection of the cells intraportally. We found that batimastat did not inhibit the extravasation of these cancer cells: at no time point were the proportions of cells at any position (intravascular, in process of extravasating, or extravascular) statistically different between the batimastat-treated and control groups.

These results challenge the widely-held belief that protease inhibitors block metastasis at the level of extravasation. Extravasation is the first obstacle faced by circulating cancer cells, and involves invasion through the basement membrane. This process of invasion is thought to require proteases and consequently could be blocked by protease inhibitors. Furthermore, these results counter the hypothesis put forth by Eccles *et al.* (42) that batimastat inhibits extravasation, based on their observation that batimastat reduced the number of lung tumor colonies by 80.4% after being administered only during

the first 72 hours of a 35-day experimental metastasis assay. Finally, these results are yet another piece of evidence originating from our research group that matrix metalloproteinase inhibitors do not inhibit extravasation. Sahadia Koop has found that, in the chick chorioallantoic membrane, B16F10 cells which have been genetically engineered to overexpress the endogenous matrix metalloproteinase inhibitor TIMP-1 do not differ in their time course of extravasation compared to parental B16F10 cells (52). Rather, TIMP-1 appeared to inhibit the growth of melanotic tumors when observed at three and seven days following cell injection.

The liver was the organ of choice for all experiments because it is a common site of metastasis in cancer patients and because of the ease in examining the liver microcirculation using IVVM. The study of possible inhibition of extravasation in the liver may raise the criticism that the liver sinusoids are unusually fenestrated; this is an organ whose primary role is the detoxification of substances in the circulation, and as such the liver sinusoids have a fenestrated endothelium and an incomplete basement membrane, in order to allow materials to pass between the circulation and the liver tissue. It is possible that this incomplete basement membrane may make extravasation easier in the liver than in other organs. However, this does not mean that all cells can extravasate. In studies of the liver by our research group using IVVM, only cells which are known to extravasate, such as leukocytes and cancer cells, have been seen to extravasate. Cells which normally do not undergo extravasation, such as erythrocytes, have never been seen to extravasate. In addition, the normal time course for the extravasation of B16F1 cells in the liver (24-48 hours) is greater than the time course observed for similar B16F10 cells in the unfenestrated chick chorioallantoic membrane microcirculation (12-24 hours) (55).

This indicates that extravasation is not unusually easy for melanoma cells trapped in the liver sinusoids. In summary, the liver microcirculation was a good model to use for this study, and the experiments demonstrated that batimastat had no effect on the time course of extravasation of B16F1 cells.

It should be noted that  $2 \times 10^5$  B16F1 cells were injected into each mouse to study extravasation, instead of the  $10^5$  B16F1 cells that were injected into each mouse for the experimental metastasis assays. Higher numbers of cells were used in the extravasation studies to increase the number of cells that could be observed in the liver sinusoids in a reasonable amount of time (1-2 hours) using IVVM. This increase in the number of cells was not believed to affect the ability of each cell to extravasate. It is possible that if very large numbers of cells were injected, which resulted in increased cell-to-cell contact and clumping of cells in the liver microcirculation such that large areas of blood flow were blocked, the ability of individual cells to extravasate might be altered. However, we did not observe large clumps of cells in the microcirculation, and most cells observed were not in contact with other cells. Thus, we believe that the increase in the number of cells injected in the extravasation assays compared to the metastasis assays did not influence the ability of individual cells to extravasate.

### **4.3 Initial Growth of Micrometastases**

Based on our observations that batimastat did not inhibit extravasation, we concluded that this compound must affect the post-extravasation growth of metastases. To summarize this logic, we have already demonstrated that batimastat is effective in reducing the mean size of liver tumors in an experimental hematogenous metastasis assay.

In this metastasis assay, the cells were injected directly into the circulation, and thus the major stages of metastasis facing the cells were extravasation, the growth of single cells into micrometastases, and continued growth requiring angiogenesis. Following our findings that batimastat did not reduce extravasation, we investigated the effect of this inhibitor on the initial growth of single cells into micrometastases.

To investigate initial growth, the proportions of micrometastases to single cancer cells were determined in 30  $\mu\text{m}$  thick sections of mouse liver prepared four days following B16F1 cell injection and subsequent to batimastat treatment. The results were unexpected: the ratio of micrometastases to single cells was over three times as high in the batimastat-treated mice as in the controls (38.9/1000 cells vs 12.0/1000 cells, respectively,  $P = 0.041$ ). This finding is opposite to what was expected: batimastat actually seemed to *promote* the formation of micrometastases. One can only speculate as to the reason(s) for this result: perhaps single cancer cells in the liver tissue perceived batimastat as a threat to survival, and in defense of this signalled themselves and perhaps other single cancer cells to start dividing. This would result in a greater subpopulation of single cancer cells that were stimulated to begin growing than was found in untreated liver tissue.

This is statistically the same situation as seen in the experimental metastasis assay where batimastat was administered in regimen 1. The number of mice in each treatment group was small (six), and the P-value was not much below 0.05 (0.041). Therefore, the same argument can be made as for that metastasis assay: it is within reason that the observed difference was due to chance variation. However, the message is clear:

batimastat does not inhibit the initial growth of single cancer cells into micrometastases. This compound must therefore inhibit a subsequent stage of growth, such as angiogenesis.

The survival of individual cancer cells in the liver was also assessed. Survival was determined by calculating the ratio of single cells to 10.2  $\mu\text{m}$  inert polystyrene microspheres in the liver sections and dividing this ratio by the ratio of single cells to microspheres in the syringe immediately following the injection of this cell:microsphere suspension into mice. Batimastat did not affect the survival of single cancer cells in the liver at four days post-injection (batimastat: 72.1% survival vs control: 88.4% survival,  $P = 0.319$ ). This result was not unexpected, for batimastat has shown a lack of direct cytotoxicity when exposed to cultured cells *in vitro* (40-42).

In assessing cancer cell survival, two major assumptions were made. The first is that every cell and microsphere injected intraportally was trapped in the liver sinusoids. This assumption is validated by the fact that the members of our research group, in studying the initial arrest of cancer cells and 10.2  $\mu\text{m}$  microspheres in the liver microcirculation using IVVM, have never observed a cell or microsphere pass through the sinusoids; all have been arrested. The second assumption is that every fluorescent green cell observed in the liver sections was viable. If a cell died, it is expected that it would have lost membrane integrity, which would have caused the fluorescent nanospheres to spill out. Only cells which appeared intact were counted.

In this initial growth study,  $2 \times 10^5$  B16F1 cells were injected per mouse, as in the extravasation assays. Again, this is more than the  $10^5$  cells which were injected per mouse in the metastasis assays. Higher numbers of cells were used in this growth study for the same reason that they were used in the extravasation study: to increase the number of

cells that could be observed in a reasonable amount of time. Occasional cell-to-cell contact was observed amongst the single cells in the sections, but in general the cells were well separated. If cellular contact was abundant, increased signalling between cells may have affected the rate at which the cells grew into micrometastases. Since cellular contact was low, we believe that the increase in the number of cells injected did not affect the ability of individual cells to grow into micrometastases.

#### **4.4 Angiogenesis**

These studies were concluded by examining the effects of batimastat on angiogenesis within metastatic liver tumors. Batimastat has demonstrated potential in inhibiting angiogenesis: Taraboletti et al. (56) observed that batimastat was able to suppress the angiogenic response (degree of vascularization) within a pellet of the reconstituted basement membrane Matrigel when this pellet was combined with cancer cell supernatant and injected subcutaneously into mice. Davies et al. (33) observed that treatment with batimastat caused primary human ovarian tumors within nude mice to be much less vascular than control tumors. Our results, too, from the experimental metastasis assay in which batimastat was administered in regimen 2, indicated that batimastat may have been inhibiting neovascularization. Batimastat caused a significant reduction in the diameter of liver tumors but did not affect the tumor number compared to controls; in addition, batimastat treatment caused a significantly greater proportion of liver tumors to fail to exceed one and two millimetres in diameter, respectively. This effect is plausibly due to the inhibition of angiogenesis, as tumors with reduced vascularization would have a more difficult time growing past one or two millimetres in diameter.

Angiogenesis was examined within liver tumors from the experimental metastasis assay, treatment regimen 2. Tumors of varying sizes were removed, sectioned, and stained with hematoxylin and eosin (H&E); this staining allowed tumor vessels to be clearly detected by the presence of red blood cells within them. Stereological examination of colour photographs of the tumors demonstrated that batimastat caused a significant reduction in tumor vascular density when tumors of similar size were compared ( $P = 0.011$ ). Therefore, it appears that angiogenesis is indeed the stage of the metastatic process which batimastat inhibits.

Qualitative assessments of the tumor photographs confirmed this conclusion. There appeared to be considerably fewer areas occupied by red blood cells in batimastat-treated tumors of all three size categories (one, two, and three millimetres in diameter). In the smaller control tumors (1-2 millimetres in diameter), cells throughout the tumors appeared viable, with distinctive borders and nuclei. Most cells within the smaller batimastat-treated tumors, though, did not appear as viable: far fewer staining nuclei could be seen, and borders between cells were less apparent. This visible reduction in cell health was likely due to reduced vascularization. Two of the smaller batimastat-treated tumors also displayed pools of red blood cells in the centre of the tumor, which was interpreted as hemorrhage. It is not clear why this hemorrhage occurred: perhaps batimastat interfered with the normal structure of endothelial cells in existing vessels, or altered the proper tubule assembly of angiogenic endothelial cells. In the larger control tumors (2-3 mm in diameter), vessels appeared less dense than in the smaller tumors, but there were still many vessels of varying sizes, including several larger ones. In the larger batimastat-treated tumors, there were strikingly fewer vessels present than in controls.

Furthermore, there were no larger vessels present in the two largest treated tumors. This is interesting, for tumors will often grow around large existing vessels. Batimastat, in addition to slowing the formation of new blood vessels, may interfere with the structure of existing vessels, causing hemorrhage and possible destruction of these vessels. This may also explain the abdominal bleeding seen in all batimastat-treated mice but in none of the control mice, in the experimental metastasis assay in which batimastat was administered in regimen 2.

In assessing angiogenesis, the presence of visible erythrocytes at low magnification was used as indication of the presence of vessels. Since single erythrocytes could readily be observed, we were confident that microvessels as well as large vessels were being detected. It is possible that some microvessels were missed due to the absence of red blood cells in the plane of the section, but because both treatment groups were scored consistently, this is not likely a factor affecting the detection of differences between the groups. Also, the first stage of vessel development, that of initial vessel assembly from endothelial cells, was not detected due to the absence of a lumen and consequently the absence of red blood cells within these structures.

This experiment was performed with a small number of tumors: only five in each treatment group. This may raise concerns about the validity of the results, even with a P-value of less than 0.05. Similar situations have been mentioned: the observations that batimastat may have increased the number of liver tumors when administered in regimen 1 and that batimastat may have increased the rate at which single cells grow into micrometastases were questioned due to small sample sizes and P-values of just under 0.05. However, in this angiogenesis assay the sample size was small, yet the P-value was

0.011, *well* under 0.05. In addition, examination of the tumor photographs showed visually striking reductions in the number of vessels and the apparent health of the cells in the batimastat-treated tumors compared to the controls.

#### **4.5 Concluding Remarks**

We have discovered that the matrix metalloproteinase inhibitor batimastat, when administered daily, is effective in reducing the average size of liver tumors in an experimental hematogenous metastasis assay performed in mice. To study this inhibition of metastasis by batimastat, we examined every major stage of the metastatic process faced by circulating cancer cells: extravasation, the initial growth of micrometastases, and angiogenesis. Our initial hypothesis was that batimastat blocked extravasation, because extravasation is the first major obstacle faced by circulating cancer cells and is believed to require proteolysis. We found that batimastat did not inhibit extravasation, nor did it inhibit initial growth. We did find, however, that batimastat caused an apparent reduction in the vascular density of 19-day liver tumors. Thus, we concluded that batimastat inhibited angiogenesis.

These studies represent the first time that anyone has examined these individual stages of the metastatic process in an attempt to determine more precisely the mechanisms of action of an anticancer drug. I believe that this study in particular will be valuable in the treatment of metastatic cancer with batimastat and its derivative marimastat. Batimastat and marimastat are currently in clinical trials in the United Kingdom, and are speculated to be valuable adjuvants to traditional cytotoxic therapy such as chemotherapy or radiation therapy. The knowledge that batimastat reduces metastasis to the liver in a

mammalian model by inhibiting angiogenesis may help to improve the dosage and timing of administration of the drug, as the therapeutic target has become more defined. I also believe that this study in general will be valuable, for it sets a precedent towards the detailed examination of other classes of antimetastatic compounds so that their mechanisms of action, and consequently their optimum therapeutic administration, can be determined.

#### **4.6 Future Considerations**

These studies should be extended to other organs, such as the lung. Based on the findings of Eccles and others that batimastat, when administered only during the first 72 hours following cancer cell injection (the period during which extravasation takes place) inhibits metastasis to the lung, it is possible that, in this organ, batimastat is inhibiting extravasation. Lung tissue is very different from liver tissue, and consequently the antimetastatic mechanisms of batimastat may be different in the two organs. Extravasation in the lung could be studied with IVVM, although with difficulty due to the movements of respiration. The lung and the liver represent two of the most common sites of metastasis clinically; consequently it would be worthwhile to study the effects of batimastat on extravasation and other steps of metastasis in the lung.

The effects of batimastat on angiogenesis should be clarified further. More tumors should be studied to increase the sample size, including tumors of sizes not yet examined, such as 0.5 and 5 millimetres in diameter. This increased sample size will also help to develop clear trends in qualitative tumor morphology between treatment groups. Different staining procedures should also be attempted, such as immunostaining with anti-

von Willebrand factor (factor VIII) antibodies, which detect endothelial cells: this may be a more reliable way to detect the presence of all tumor blood vessels, including those which have not yet formed a lumen.

Tests should be performed to determine if batimastat increases the rate of apoptosis within liver tumors. Apoptosis, or programmed cell death, is another mechanism by which some anticancer drugs may work. In addition, the effects of batimastat on the rate of proliferation of cells within liver tumors should be determined. Much work remains to be done in order to determine the true potential of batimastat and other protease inhibitors in inhibiting the metastatic process.

**APPENDIX: ETHICS APPROVAL LETTERS, 1994-1997****1994 ETHICS APPROVAL**

March 11, 1994

Dear Dr. Morris:

Your "Application to Use Animals for Research or Teaching" entitled:

**"Molecular and In Vivo Videomicroscopic Analysis of Mechanism of Cancer Metastasis"**

has been approved by the University Council on Animal Care. This approval expires in one year on the last day of the month. The number for this project is # 84071-3

1. This number must be indicated when ordering animals for this project.
2. Animals for other projects may not be ordered under this number.
3. If no number appears on this approval please contact this office when grant approval is received. If the application for funding is not successful and if you wish to proceed with the project, request that an internal scientific peer review be performed by your animal care committee.
4. Purchases of animals other than through this system must be cleared through the ACVS office. Health certificates will be required.

**ANIMALS APPROVED**

Mice - Balb/C NU/NU - 200; C57/BL - 200; C3H - 100; GR - 20; Balb/C - 20  
Chicken Eggs (Fertilized) - 30 doz.

**REQUIREMENTS/COMMENTS**

Please ensure that individual(s) performing procedures, as described in this protocol, are familiar with the contents of this document.

If the cell lines indicated are to be used at LRCC the possibility of them being contaminated with MHV should be addressed.

c.c. A. Hryciak  
A. Parbtani  
P. Cookwell



*Handwritten signature/initials*

**A. Hyatt  
Office of Research Services**

1. Recommend using an absorbent suture for closing the muscle layer (Vicryl 3-0. See ACVS for supplies.
2. Recommend an antibiotic after all recovery surgeries. Supranorbine can be administered at the dosage 0.05 - 0.1 mg/kg subcutaneously every 12 hours. Give it dose at the end of surgery and the other ½ when animal is recovering.
3. The graduate course on animal care will be offered in May.
4. Please ensure mice are never left unattended during video microscopy.
5. Subcutaneous fluids can be administered after surgery and during video microscopy to keep animals moist. Administer 2-3 ml of warm sterile saline under the scruff.

Please ensure that individual(s) performing procedure, as described in this protocol, are familiar with the contents of this document.

**REQUIREMENTS/COMMENTS**

Mice - Albino or Balb/c - 200; C57/BL - 100; GR - 20; C3H - 20; NIH Swiss - 20  
Chicken Eggs (Fertilized) - 30 dozen

**ANIMALS APPROVED**

1. This number must be indicated when ordering animals for this project.
2. Animals for other projects may not be ordered under this number.
3. If no number appears on this approval please contact this office when grant approval is received. If the application for funding is not successful and if you wish to proceed with the project, request that an internal schedule review be performed by your animal care committee.
4. Purchases of animals other than through this system must be cleared through the ACVS office. Health certificates will be required.

has been approved by the University Council on Animal Care. This approval expires in one year on the last day of the month. The number for the project is # 1995-3

**"Molecular and In Vivo Videomicroscopic Analysis of Mechanisms of Cancer Metastasis"**  
Funding Agency: National Cancer Institute - NCI

Your "Application to Use Animals for Research or Teaching" entitled:

Dear Dr. Morris:

March 30, 1995

**Council on Animal Care • Animal Care and Veterinary Services  
Director - Michele M. Bailey, D.V.M.  
Clinical Veterinarian - Susan H. Fernald, D.V.M.**

**The University of Western Ontario**



**1995 ETHICS APPROVAL**

## 1996 ETHICS APPROVAL



## The UNIVERSITY of WESTERN ONTARIO

University Council on Animal Care  
Animal Use Subcommittee

March 6, 1996

Dear Dr. Morris:

Your "Application to Use Animals for Research or Teaching" entitled:

"Molecular and In Vivo Videomicroscopic Analysis of Mechanisms of Cancer Metastasis"  
Funding Agency: NSCI

has been approved by the University Council on Animal Care. This approval expires in one year on the last day of the month. The number for this project is # 9051-3. This replaces #9005-3.

1. This number must be indicated when ordering animals for this project.
2. Animals for other projects may not be ordered under this number.
3. If no number appears on this approval please contact this office when grant approval is received. If the application for funding is not successful and if you wish to proceed with the project, request that an internal scientific peer review be performed by your animal care committee.
4. Purchases of animals other than through this system must be cleared through the AGIS office. Health certificates will be required.

ANIMALS APPROVED

Mice	na/na	-	4-8 wks, F	-	100
	B6h/C	-	4-8 wks, F	-	100
	CS7/B1	-	4-8 wks, F	-	100
	GR	-	4-8 wks, F	-	20
	CSH	-	4-8 wks, F	-	20
	MDH Strain	-	4-8 wks, F	-	20
	CD-1 (HE)	-	6-8 wks, M/F	-	10
	Chicken eggs	-	N/F	-	30 dozen

REQUIREMENTS/COMMENTS

~~Please ensure that individual IACUC reviewing procedures as described in this protocol are met through the contacts of this document.~~

Procedures in this protocol should be carried out according to the following SOPs. Please contact the Animal Use Subcommittee office (661-2111 ext. 6770) in case of difficulties or if you require copies.

SOPs	#100-01:	"Housing/Tumor Growth/Animals"
	#310-01:	"Holding Period Post-Adaptation"
	#320-01:	"Euthanasia"
	#321-01:	"Criteria for Early Euthanasia/Animals"
	#330-01:	"Post-Operative Care - Rodent"
	#340-01:	"Surgical Prep/Rodent/Clean"

c.c. Approved Renewal - V. Morris  
Approval Letter - K. Perry

## 1997 ETHICS APPROVAL



## The UNIVERSITY of WESTERN ONTARIO

University Council on Animal Care  
Animal Use Subcommittee

March 27, 1997

Dear Dr. Morris:

Your "Application to Use Animals for Research or Teaching" entitled:

"Steps in Metastasis: Identifying Therapeutic Targets"  
Funding Agency: NIH

has been approved by the University Council on Animal Care. This approval expires in one year on the last day of the month. The number for this project is # 97057-3. This replaces #96051-3.

1. This number must be indicated when ordering animals for this project.
2. Animals for other projects may not be ordered under this number.
3. If no number appears on this approval please contact this office when grant approval is received. If the application for funding is not successful and if you wish to proceed with the project, request that an interval scientific peer review be performed by your animal care committee.
4. Purchases of animals other than through this system must be cleared through the ACVS office. Health certificates will be required.

ANIMALS APPROVED

Non	-	SCID, 4-8 wks, F	-	250
	-	nu/nu, 4-8 wks, F	-	250
	-	BALB/C, 4-8 wks, F	-	100
	-	CS7/NL, 4-8 wks, F	-	250
	-	CE, 4-8 wks, F	-	20
	-	CH, 4-8 wks, F	-	20
	-	NDN Strain, 4-8 wks, F	-	20
	-	CD-1 (HE), 4-8 wks, F	-	20
	-	Chicken Eggs, fertilized	-	30 dozen

REQUIREMENTS/COMMENTS

~~Please ensure that all laboratory procedures, animal care, and facilities with the committee's approval.~~

Procedures in this protocol must be carried out according to the following SOPs. Please contact the Animal Use Subcommittee office (867-2111 ext. 6770) in case of difficulties or if you require copies.

SOPs	#100-01:	"Housing/Tissue Growth/Reagents"
	#110-01:	"Holding Period Post-Admission"
	#300-01:	"Euthanasia"
	#321-01:	"Criteria for Early Euthanasia/Reagents"
	#330-01:	"Post-Operative Care - Rats"
	#340-01:	"Surgical Prep/Reagent/Class"

1. Please ensure that the old protocol number (#96051-3) is replaced by the new protocol number (#97057-3) on all pertinent animal records, cards, door signs, etc. All personnel ordering animals must also be informed of this new protocol number.

2. Please monitor the number of animals used in 1997-98 in order to more readily project future animal needs.

c.c. Approved Protocol - V. Morris, P. Costwell  
Approval Letter - P. Gilmartin, K. Perry  
Costwell

## References

1. National Cancer Institute of Canada: **Canadian Cancer Statistics 1996**. Toronto, Canada, 1996.
2. Liotta LA. Tumor invasion and metastases: role of the basement membrane. *Am J Path* 1984; 117(3): 339-348.
3. Weiss L and Schmid-Schonbein GW. Biomechanical interactions of cancer cells with the microvasculature during metastasis. *Cell Biophysics* 1989; 14: 187-215.
4. Fidler IJ. Invasion and Metastasis. In: Abeloff MD, Armitage JO, Lichter AS, Niederhuber JE, editors. *Clinical Oncology*. New York: Churchill Livingstone, 1995: 55-76.
5. Folkman J. Tumour angiogenesis. *Adv Cancer Res* 1985; 43: 175-203.
6. Fidler IJ. Metastasis: quantitative analysis of distribution and fate of tumor emboli labeled with <sup>125</sup>I-5-iodo-2'-deoxyuridine. *J Natl Cancer Inst* 1970; 45: 773-782.
7. Weiss L. Metastatic inefficiency. *Adv Cancer Res* 1990; 54: 193-211.
8. Powell WC and Matrisian LM. Complex roles of matrix metalloproteinases in tumor progression. In: Gunthert U, Birchmeier W, editors. *Attempts to understand metastasis formation I: Metastasis-related molecules*. Berlin: Springer-Verlag, 1996: 1-21.
9. Puente XS, Pendas AM, Llano E, Velasco G, and Lopez-Otin C. Molecular cloning of a novel membrane-type matrix metalloproteinase from a human breast carcinoma. *Cancer Res* 1996; 56: 944-949.
10. Cossins J, Dudgeon TJ, Catlin G, Gearing AJH, and Clements JM. Identification of MMP-18, a putative novel human matrix metalloproteinase. *Biochem Biophys Res Commun* 1996; 228: 494-498.
11. DeClerck YA and Imren S. Protease inhibitors: role and potential therapeutic use in human cancer. *Eur J Cancer* 1994; 30A(14): 2170-2180.
12. Kohn EC and Liotta LA. Molecular insights into cancer invasion: strategies for prevention and intervention. *Cancer Res* 1995; 55: 1856-1862.
13. Mignatti P and Rifkin DB. Biology and biochemistry of proteinases in tumor invasion. *Physiological Reviews* 1993; 73(1): 161-195.

14. Liotta LA, Steeg PS, and Stetler-Stevenson WG. Cancer metastasis and angiogenesis: an imbalance of positive and negative regulation. *Cell* 1991; 64: 327-336.
15. Birkedal-Hansen H, Moore WGI, Bodden MK, Windsor LJ, Birkedal-Hansen B, DeCarlo A, and Engler JA. Matrix metalloproteinases: a review. *Crit Rev Oral Bio Med* 1993; 4(2): 197-250.
16. Agren MS, Taplin CJ, Woessner JF, Eaglstein WH, and Mertz PM. Collagenase activity during wound-healing. *J Invest Dermatol* 1992; 98: 621-621.
17. Reponen P, Sahlberg C, Huhtala P, Hurskainen T, Thesleff I, and Tryggvason K. Molecular cloning of murine 72-kDa type IV collagenase and its expression during mouse development. *J Biol Chem* 1992; 267: 7856-7862.
18. Woessner, Jr. JF. Matrix metalloproteinases and their inhibitors in connective tissue remodeling. *FASEB* 1991; 5: 2145-2154.
19. MacDougall JR and Matrisian LM. Contributions of tumor and stromal matrix metalloproteinases to tumor progression, invasion and metastasis. *Cancer and Metastasis Reviews* 1995; 14: 351-362.
20. Clavel C, Polette M, Doco M, Binniger I, and Birembaut P. Immunolocalization of matrix metallo-proteinases and their tissue inhibitor in human mammary pathology. *Bull Cancer (Paris)* 1992; 79: 261-270.
21. Basset P, Bellocq JP, Wolf C, Stoll I, Hutin P, Limacher JM, Podhajcer OL, Chenard MP, Rio MC, and Chambon P. A novel metalloproteinase gene specifically expressed in stromal cells of breast carcinoma. *Nature* 1990; 348: 699-704.
22. Stearns ME and Wang M. Type IV collagenase (M<sub>r</sub> 72,000) expression in human prostate: benign and malignant tissue. *Cancer Res* 1993; 53: 878-883.
23. Powell WC, Knox JD, Navre M, Grogan TM, Kittelson J, Nagle RB, and Bowden GT. Expression of the metalloproteinase matrilysin in DU-145 cells increases their invasive potential in severe combined immunodeficient mice. *Cancer Res* 1993; 53: 417-422.
24. Poulson R, Pignatelli M, Stetler-Stevenson WG, Liotta LA, Wright PA, Jeffery RE, Longcroft JM, Rogers L, and Stamp GW. Stromal expression of 72 kDa type IV collagenase (MMP-2) and TIMP-2 mRNAs in colorectal neoplasia. *Am J Pathol* 1992; 141: 389-396.
25. Urbanski SJ, Edwards DR, Maitland A, Leco KJ, Watson A, and Kossalowska AE. Expression of metalloproteinases and their inhibitors in primary pulmonary carcinomas. *Br J Cancer* 1992; 66: 1188-1194.

26. Sato H, Takino T, Okada Y, Cao J, Shinagawa A, Yamamoto E, and Seiki M. A matrix metalloproteinase expressed on the surface of invasive tumour cells. *Nature* 1994; 370: 61-65.
27. Campo E, Merino MJ, Tavassoli FA, Charonis AS, Stetler-Stevenson WG, and Liotta LA. Evaluation of basement membrane components and the 72 kDa type IV collagenase in serous tumors of the ovary. *Am J Surg Pathol* 1992; 16: 500-507.
28. Campo E, Merino MJ, Liotta LA, Neumann R, and Stetler-Stevenson, WG. Distribution of the 72-kd type IV collagenase in nonneoplastic and neoplastic thyroid tissue. *Human Pathol* 1992; 23: 1395-1401.
29. Ura H, Bonfil D, Reich R, Reddel R, Pfeifer A, Harris CC, and Klein-Szanto AJP. Expression of type IV collagenase and procollagen genes and its correlation with the tumorigenic, invasive, and metastatic abilities of oncogene-transformed human bronchial epithelial cells. *Cancer Res* 1989; 49: 4615-4621.
30. Monteagudo C, Merino MJ, San-Juan J, Liotta LA, and Stetler-Stevenson WG. Immunohistochemical distribution of type IV collagenase in normal, benign, and malignant breast tissue. *Am J Pathol* 1990; 136(3): 585-592.
31. Levy AT, Ciocco V, Sobel ME, Garbisa S, Grigioni, WF, Liotta LA, and Stetler-Stevenson WG. Increased expression of the  $M_r$  72,000 type IV collagenase in human colonic adenocarcinoma. *Cancer Res* 1991; 51: 439-444.
32. Stetler-Stevenson WG, Liotta LA, and Kleiner, Jr. DE. Extracellular matrix 6: role of matrix metalloproteinases in tumor invasion and metastasis. *FASEB* 1993; 7: 1434-1441.
33. Davies B, Brown PD, East N, Crimmin MJ, and Balkwill FR. A synthetic matrix metalloproteinase inhibitor decreases tumor burden and prolongs survival of mice bearing human ovarian carcinoma xenografts. *Cancer Res* 1993; 53: 2087-2091.
34. Fisher C, Gilbertson-Beadling S, Powers EA, Petzold G, Poorman R, and Mitchell MA. Interstitial collagenase is required for angiogenesis *in vitro*. *Developmental Biology* 1994; 162: 499-510.
35. Galardy RE, Grobelny D, Foellmer HG, and Fernandez LA. Inhibition of angiogenesis by the matrix metalloproteinase inhibitor N-[2R-2-(hydroxyamidocarbonylmethyl)-4-methylpentanoyl]-L-tryptophan methylamide. *Cancer Res* 1994; 54: 4715-4718.
36. Brown PD. Matrix metalloproteinase inhibitors: a novel class of anticancer agents. *Advan Enzyme Regul* 1995; 35: 293-301.

37. Botos I, Scapozza L, Zhang D, Liotta LA, and Meyer EF. Batimastat, a potent matrix metalloproteinase inhibitor, exhibits an unexpected mode of binding. *Proc Natl Acad Sci USA* 1996; 93: 2749-2754.
38. Sledge, Jr. GW, Qulali M, Goulet R, Bone EA, and Fife R. Effect of matrix metalloproteinase inhibitor batimastat on breast cancer regrowth and metastasis in athymic mice. *J Natl Cancer Inst* 1995; 87(20): 1546-1550.
39. Wang X, Fu X, Brown PD, Crimmin MJ, and Hoffman RM. Matrix metalloproteinase inhibitor BB-94 (batimastat) inhibits human colon tumor growth and spread in a patient-like orthotopic model in nude mice. *Cancer Res* 1994; 54: 4726-4728.
40. Chirivi RGS, Garofalo A, Crimmin MJ, Bawden LJ, Stoppacciaro A, Brown PD, and Giavazzi R. Inhibition of the metastatic spread and growth of B16-BL6 murine melanoma by a synthetic matrix metalloproteinase inhibitor. *Int J Cancer* 1994; 58: 460-464.
41. Watson SA, Morris TM, Robinson G, Crimmin MJ, Brown PD, and Hardcastle JD. Inhibition of organ invasion by the matrix metalloproteinase inhibitor batimastat (BB-94) in two human colon carcinoma metastasis models. *Cancer Res* 1995; 55: 3629-3633.
42. Eccles SA, Box GM, Court WJ, Bone EA, Thomas W, and Brown PD. Control of lymphatic and hematogenous metastasis of a rat mammary carcinoma by the matrix metalloproteinase inhibitor batimastat (BB-94). *Cancer Res* 1996; 56: 2815-2822.
43. Gore M, Hern RA, Stankiewicz M, Slevin M, Millar A, Brown P, Cornish A, and Baillet M. Tumor marker levels during marimastat therapy. *Lancet* 1996; 348: 263-264.
44. Malfetano J, Teng N, and Moore D. Marimastat, a novel matrix metalloproteinase inhibitor in patients with advanced cancer of the ovary: a dose-finding study. *Proc Am Soc Clin Oncol* 1996; 15: 283 (abstr 764).
45. Boasberg P, Harvaugh B, and Roth B. Marimastat, a novel matrix metalloproteinase inhibitor in patients with hormone-refractory prostate cancer. *Proc Am Soc Clin Oncol* 1996; 15: 258 (abstr 671).
46. Rosemurgy A, Harris J, Langleben A, Casper E, Allen R, and Rasmussen H. Marimastat, a novel matrix metalloproteinase inhibitor in patients with advanced carcinoma of the pancreas. *Proc Am Soc Clin Oncol* 1996; 15: 207 (abstr 470).
47. Liotta LA. Tumor invasion and metastases: role of the extracellular matrix. *Cancer Res* 1986; 46: 1-7.

48. Liotta LA, Tryggvason K, Garbisa S, Hart I, Foltz CM, and Shafie S. Metastatic potential correlates with enzymatic degradation of basement membrane collagen. *Nature* 1980; 284: 67-68.
49. MacDonald IC, Schmidt EE, Morris VL, Chambers AF, and Groom AC. Intravital videomicroscopy of the chorioallantoic microcirculation: a model system for studying metastasis. *Microvasc Res* 1992; 44: 185-199.
50. Chambers AC, Schmidt EE, MacDonald IC, Morris VL, and Groom AC. Early steps in hematogenous metastasis of B16F1 melanoma cells in chick embryos studied by high-resolution videomicroscopy. *J Natl Cancer Inst* 1992; 84(10): 797-803.
51. Morris VL, MacDonald IC, Koop S, Schmidt EE, Chambers AC, and Groom AC. Early interactions of cancer cells with the microvasculature in mouse liver and muscle during hematogenous metastasis: videomicroscopic analysis. *Clin Exp Metastasis* 1993; 11: 377-390.
52. Koop S, Khokha R, Schmidt EE, MacDonald IC, Morris VL, Chambers, AF, and Groom AC. Overexpression of metalloproteinase inhibitor in B16F1 cells does not affect extravasation but reduces tumor growth. *Cancer Res* 1994; 54: 4791-4797.
53. Morris VL, Koop S, MacDonald IC, Schmidt EE, Grattan M, Percy D, Chambers AF, and Groom AC. Mammary carcinoma cell lines of high and low metastatic potential differ not in extravasation but in subsequent migration and growth. *Clin Exp Metastasis* 1994; 12: 357-367.
54. Morris VL, Schmidt EE, Koop S, MacDonald IC, Grattan M, Khokha R, McLane MA, Niewiarowski S, Chambers AF, and Groom AC. Effects of the disintegrin eristostatin on individual steps of hematogenous metastasis. *Exp Cell Res* 1995; 219: 571-578.
55. Koop S, MacDonald IC, Luzzi K, Schmidt EE, Morris VL, Grattan M, Khokha R, Chambers AF, and Groom AC. Fate of melanoma cells entering the microcirculation: over 80% survive and extravasate. *Cancer Res* 1995; 55: 2520-2523.
56. Taraboletti G, Garofalo A, Belotti D, Drudis T, Borsotti P, Scanziani E, Brown PD, and Giavazzi R. Inhibition of angiogenesis and murine hemangioma growth by batimastat, a synthetic inhibitor of matrix metalloproteinases. *J Natl Cancer Inst* 1995; 87(4): 293-298.